Circadian rhythms of macrophages are altered by the acidic pH of the tumor microenvironment.

Amelia M. Knudsen-Clark[1], Daniel Mwangi[2], Juliana Cazarin[2], Kristina Morris[2], Cameron Baker[3], Lauren M. Hablitz[4], Matthew N. McCall[2,5,6], Minsoo Kim[1,6], Brian J. Altman[2,6,*].

[1]Department of Microbiology and Immunology, [2]Department of Biomedical Genetics, [3]Genomics Research Center, [4]Center for Translational Neuromedicine, [5]Department of Biostatistics and Computational Biology, and [6]Wilmot Cancer Institute, University of Rochester Medical Center, Rochester, New York, USA.

*Corresponding author.

E-mail: Brian_Altman@URMC.rochester.edu

Abstract

Macrophages are prime therapeutic targets due to their pro-tumorigenic and immunosuppressive functions in tumors, but the varying efficacy of therapeutic approaches targeting macrophages highlights our incomplete understanding of how the tumor microenvironment (TME) can influence regulation of macrophages. The circadian clock is a key internal regulator of macrophage function, but how circadian rhythms of macrophages may be influenced by the tumor microenvironment remains unknown. We found that conditions associated with the TME such as polarizing stimuli, acidic pH, and elevated lactate concentrations can each alter circadian rhythms in macrophages. Circadian rhythms were enhanced in pro-resolution macrophages but suppressed in pro-inflammatory macrophages, and acidic pH had divergent effects on circadian rhythms depending on macrophage phenotype. While cyclic AMP (cAMP) has been reported to play a role in macrophage response to acidic pH, our results indicate that pH-driven

25 changes in circadian rhythms are not mediated solely by the cAMP signaling pathway. Remarkably, clock
26 correlation distance analysis of tumor-associated macrophages (TAMs) revealed evidence of circadian
27 disorder in TAMs. This is the first report providing evidence that circadian rhythms of macrophages are
28 altered within the TME. Our data further suggest that heterogeneity in circadian rhythms at the
29 population level may underlie this circadian disorder. Finally, we sought to determine how circadian
30 regulation of macrophages impacts tumorigenesis, and found that tumor growth was suppressed when
31 macrophages had a functional circadian clock. Our work demonstrates a novel mechanism by which the
32 tumor microenvironment can influence macrophage biology through altering circadian rhythms, and the
33 contribution of circadian rhythms in macrophages to suppressing tumor growth.

Introduction

Tumor-associated macrophages (TAMs) are one of the most abundant leukocytes found in solid tumors, with high intra-tumoral TAM density generally associated with poor clinical outcome [1-3]. This is consistent with the largely pro-tumorigenic role of macrophages within tumors[4]. Macrophages are highly plastic professional phagocytes whose ability to sense and respond to the environment makes them uniquely equipped to protect tissue integrity under normal homeostatic conditions[5, 6]. However, within the chronically inflamed tumor microenvironment (TME), failure to resolve the inflammation can lead to uncontrolled secretion of tissue repair factors by TAMs, promoting tumor growth and metastatic capacity[7-9]. At the same time, conditions in the TME can drive TAMs to suppress potentially anti-tumorigenic inflammatory activity through various mechanisms including secretion of anti-inflammatory cytokines and expression of checkpoint inhibitors such as PD-L1, promoting immune suppression[4, 10-16].

TAMs are known to suppress the response to many standard of care treatments through their pro-tumorigenic and immunosuppressive functions, making them a prime therapeutic target[17]. However, we still have an incomplete understanding of how the TME influences macrophages, limiting our ability to target them; this is highlighted by the varying efficacy of therapeutic approaches used to target macrophages[18]. This is thought to be due in part to the significant phenotypic heterogeneity of TAMs within tumors[18-20]. Evidence suggests this heterogeneity is due to the ability of macrophages to sense and adapt to the local microenvironment, which varies within tumors depending on several factors including the distance from blood vessels and neighboring cells[21-24]. Indeed, various conditions in the TME have been shown to influence macrophage phenotype and function[4].

58 In particular, poor vascularization of solid tumors leads to inefficient delivery of oxygen, creating regions
59 of hypoxia[25]. The hypoxic response promotes enhanced glycolytic activity of cells within the region,
60 which, coupled with poor tissue drainage as a result of leaky vasculature, results in elevated levels of
61 protons and lactate, acidifying the microenvironment[26, 27]. Of conditions in the TME, it has been well
62 appreciated that acidic (low) pH can promote a pro-resolution phenotype, thereby contributing to the
63 pro-tumorigenic and immunosuppressive functions of macrophages within tumors[28-30].
64
65 The myriad ways in which the TME can impact regulation of macrophages remain to be fully elucidated.
66 Circadian rhythms are a key regulatory system present in almost all cells of the body, and are an
67 understudied facet of macrophage biology[31]. Acidic pH is a condition commonly associated with the
68 TME that has been shown to alter circadian rhythms in cell lines[32]; however, whether pH influences
69 circadian rhythms in macrophages remain unknown.
70
71 Circadian rhythms are 24-hour rhythms that impart oscillations in the levels of circadian-regulated gene
72 transcripts and proteins in a tissue- and cell-specific manner, resulting in time-of-day-dependent variation
73 in many cellular processes[33, 34]. The molecular clock, which we will refer to as the circadian clock, drives
74 these rhythms in cells through a cell-autonomous transcription/translation feedback loop, which is
75 controlled in part by the transcription factor BMAL1[31]. Circadian clocks are synchronized by signals sent
76 out from the central circadian clock housed within the suprachiasmatic nucleus of the hypothalamus,
77 which entrains circadian clocks to the time of day[31]. This allows for the temporal coordination of cells in
78 spatially distinct tissues, although how the local microenvironment influences circadian rhythms remains
79 to be elucidated.
80

81 All leukocytes tested to date have functional circadian clocks[35-42]. As such, nearly every arm of the
82 immune response (both innate and adaptive) is subject to circadian regulation[35, 37, 43]. Time-of-day-
83 dependent regulation of immune responses is achieved though temporal gating of response to stimuli,
84 effector function, and cell trafficking[42, 44-48], all of which promote coordination between the multiple
85 phases of the immune response[40, 42, 49-53].
86
87 Key aspects of macrophage function are subject to circadian regulation, including cytokine secretion and
88 phagocytosis[36, 44, 45, 51, 54]. This results in a time-of-day-dependent macrophage response to
89 stimuli, which modulates the magnitude of the resulting adaptive immune response and determines
90 disease progression[44, 51, 55]. Circadian regulation of macrophages is of particular interest given recent
91 evidence of 24-hour circadian variation in the frequency of TAMs expressing surface markers associated
92 with pro- or anti-tumorigenic phenotypes[56-58]. A promising application of such circadian variation was
93 made evident in leveraging observations of circadian frequency in TAMs expressing immune checkpoint
94 blockade (ICB) target PD-1 to increase efficacy of PD-1/PD-L1 ICB therapy by timing treatment to the
95 time of day when PD-1+ TAMs were most frequent[57, 59]. This suggests that leveraging time-of-day
96 variations in therapeutic targets could be a promising avenue to increase efficacy, highlighting the
97 importance of understanding how circadian rhythms of macrophages may be influenced by conditions in
98 the TME, which remains unclear.
99
100 In this work, we present evidence that circadian rhythms of macrophages are altered in the TME. We
101 uncover a novel way in which two conditions within the TME, acidic pH and lactate, can influence
102 macrophage biology through modulation of circadian rhythms. We also find that macrophages of
103 different phenotypes have distinct circadian rhythms. Remarkably, we found evidence of circadian
104 disorder in tumor-associated macrophages, indicating that circadian rhythms are altered in macrophages

within the TME. Furthermore, our data suggest that heterogeneity in circadian rhythms at the population level may underlie the observed circadian disorder. This work elucidates a novel way in which the TME can alter macrophage biology, and represents the first steps to understanding how the tumor microenvironment can alter circadian rhythms of immune cells such as macrophages.

Results

Macrophages of different phenotypes exhibit different circadian rhythms.

As macrophages are a phenotypically heterogeneous population in the TME, we first sought to understand whether diversity in macrophage phenotype could translate to diversity in circadian rhythms of macrophages. To this end, we used two well-established *in vitro* polarization models to study distinct macrophage phenotypes[5, 60-63]. For a model of pro-inflammatory macrophages, we stimulated macrophages with interferon gamma (IFNγ) and lipopolysaccharide (LPS) to elicit a pro-inflammatory phenotype[60, 64]. These macrophages are often referred to as 'M1' and are broadly viewed as anti-tumorigenic, and we will refer to them throughout this paper as pro-inflammatory macrophages[65, 66]. For a model at the opposite end of the phenotypic spectrum, we stimulated macrophages with IL-4 and IL-13[60, 67]. While these type 2 stimuli play a role in the response to parasites and allergy, they are also major drivers of wound healing; in line with this, IL-4 and IL-13-stimulated macrophages have been well-characterized to adopt gene expression profiles associated with wound-healing and anti-inflammatory macrophage phenotypes[68-71]. As such, these macrophages are often used as a model to study pro-tumorigenic macrophages *in vitro* and are often referred to as 'M2' macrophages; throughout this paper, we will refer to IL-4 and IL-13-stimulated macrophages as pro-resolution macrophages[66, 72, 73]. Consistent with previous studies, we found that genes associated with anti-inflammatory and pro-

129 resolution programming characteristic of IL-4 and IL-13-stimulated macrophages such as *Arg1, Retnla,*
130 *Chil3* (Ym1), *Clec10a* (MGL1)*, and Mrc1 (*CD206*)* were induced in IL-4 and IL-13-stimulated macrophages,
131 but not IFNγ and LPS-stimulated macrophages. In contrast, genes associated with pro-inflammatory
132 activity characteristic of IFNγ and LPS-stimulated macrophages such as *Nos2* (iNOS)*, Tnfa, Il1b, and Il6*
133 were induced in IFNγ and LPS-stimulated macrophages, but not IL-4 and IL-13-stimulated macrophages
134 (Supplementary Figure 1)[28, 30, 65, 71, 74, 75]. This indicates that macrophages stimulated with IL-4
135 and IL-13 were polarized toward a pro-resolution phenotype, while macrophages stimulated with IFNγ
136 and LPS were polarized toward a pro-inflammatory phenotype.
137
138 Circadian rhythms of macrophages were measured by monitoring PER2, a key component of the
139 circadian clock, via the rhythmic activity of the PER2-Luciferase (PER2-Luc) fusion protein in a live cell
140 LumiCycle luminometer (Supplementary Figure 2A)[76]. Bone marrow-derived macrophages (BMDMs)
141 were generated from bone marrow of mice expressing PER2-Luc. Following differentiation, the circadian
142 clocks of BMDMs were synchronized by a 24-hour period of serum starvation followed by 2 hours of
143 serum shock[77], and rhythms were observed for up to 4 days (Supplementary Figure 2B,C).
144
145 To determine whether phenotype can influence circadian rhythms in macrophages, BMDMs were
146 cultured in the presence or absence of polarizing stimuli, and rhythms were observed by LumiCycle
147 (Figure 1). The amplitude of rhythms is the magnitude of change between the peak and the trough, and
148 is indicative of the strength of rhythms[78, 79]. Amplitude of rhythms was suppressed in pro-
149 inflammatory macrophages compared to unstimulated macrophages. In contrast, amplitude of rhythms
150 in pro-resolution macrophages was enhanced. This suggests that rhythms are suppressed in pro-
151 inflammatory macrophages but enhanced in pro-resolution macrophages, which agrees with previous
152 observations[80, 81]. Period is the amount of time it takes to complete one full oscillation[82].

153 Compared to unstimulated macrophages, period was lengthened in pro-resolution macrophages but
154 shortened in pro-inflammatory macrophages. This In line with others' observations and suggests that the
155 clock runs with a longer period (slower) in pro-resolution macrophages but runs with a shorter period
156 (faster) in pro-inflammatory macrophages[80, 81].
157
158 Interestingly, we observed differences in damping of rhythms in polarized macrophages. Damping is
159 measured as the number of days required for the amplitude of rhythms to decrease by 30% of the first
160 cycle[83]. Damping of rhythms in most free-running cell populations (defined as cells cultured in the
161 absence of external synchronizing stimuli) occurs naturally as the circadian clocks of individual cells in
162 the population become desynchronized from each other; thus, damping can be indicative of
163 desynchrony within a population[84]. The damping rate increases as the time it takes for rhythms to
164 dissipate decreases; conversely, as damping rate decreases as the time it takes for rhythms to dissipate
165 increases. We observed increased rate of damping in pro-inflammatory macrophages compared to
166 unstimulated macrophages (Figure 1), indicating that population-level rhythms were maintained for a
167 shorter length of time in pro-inflammatory macrophages. In contrast, damping rate was decreased in
168 pro-resolution macrophages, indicating that population-level rhythms were maintained for longer in pro-
169 resolution macrophages. These data suggest that pro-inflammatory macrophages may have an impaired
170 ability to maintain synchrony, while pro-resolution macrophages may have an enhanced ability to
171 maintain synchrony.
172
173 Collectively, these data suggest that pro-inflammatory macrophages have weaker rhythms and impaired
174 ability to maintain synchrony, while pro-resolution macrophages have enhanced rhythms and an
175 increased ability to maintain synchrony. This is evidence that macrophages of different phenotypes have

176 distinct circadian rhythms, suggesting that diversity of macrophage phenotype may lead to diversity in
177 macrophage circadian rhythms.
178
179 **Acidic pH alters circadian rhythms of macrophages.**
180
181 The TME has previously been shown to be acidic, with a pH ranging from 6.8 to 6.3; much more acidic
182 than the typical pH in blood and healthy tissue of 7.3-7.4[85-87]. It was previously reported that acidic
183 pH can alter circadian rhythms, but whether this applies to macrophages remains unknown[32]. Thus,
184 we cultured BMDMs under conditions of varying pH within a range that mimics that found within the
185 TME (pH6.5-pH7.4). As macrophages are a heterogeneous population in the TME, we assessed the
186 influence of acidic pH on rhythms of unstimulated, pro-resolution, and pro-inflammatory macrophages.
187 In line with previous observations, macrophages cultured at pH 6.5 were polarized toward a pro-
188 resolution phenotype, characterized by increased expression of *Arg1* and *Vegf* compared to
189 macrophages cultured at pH 7.4 (Supplementary Figure 3A). Pro-inflammatory macrophages cultured at
190 pH 6.5 had decreased expression of *Nos2* compared to those cultured at pH 7.4, suggesting that an
191 acidic pH of 6.5 both promotes a pro-resolution phenotype and suppresses a pro-inflammatory
192 phenotype.
193
194 It has been observed that inducible cyclic AMP early repressor (*Icer*), an isoform of cyclic AMP (cAMP)-
195 response modulator (*Crem*), is upregulated downstream of acid-sensing in macrophages, and has been
196 used as a "biomarker" for macrophages exposed to acidic conditions in tumors. We observed induction
197 of *Icer* in unstimulated and pro-resolution macrophages cultured at pH 6.5 compared to pH 7.4,
198 indicating that these macrophages were sensing acidic conditions (Supplementary Figure 3B). In line with
199 previous observations that *Icer* is induced downstream of LPS-driven TLR4 signaling, *Icer* was also

200 upregulated in pro-inflammatory macrophages compared to unstimulated macrophages even at neutral
201 pH 7.4[88]. Although *Icer* was not further upregulated in pro-inflammatory macrophages at pH 6.5
202 compared to pH 7.4, *Nos2* was suppressed at pH 6.5 compared to pH 7.4, suggesting that pro-
203 inflammatory macrophages responded to acidic pH. In all, these data confirm that macrophages of
204 various phenotypes can sense and respond to acidic conditions within the range of pH found in the TME.
205
206 To determine whether an acidic microenvironment can influence circadian rhythms in macrophages, we
207 assessed rhythms of unstimulated, pro-resolution, and pro-inflammatory macrophages under normal
208 and acidic conditions. To this end, BMDMs were polarized toward a pro-resolution or a pro-inflammatory
209 phenotype, or left unstimulated, and cultured in media at a normal pH of 7.4 or at acidic pH of 6.8 or 6.5;
210 PER2-Luc rhythms were then observed by LumiCycle. In unstimulated and pro-resolution BMDMs, lower
211 pH led to enhanced amplitude, a shortening in period, and increased damping rate of rhythms at pH 6.8
212 and pH 6.5 relative to neutral pH 7.4 (Figure 2A,B; Supplementary Figure 4A). This suggests that in
213 unstimulated and pro-resolution macrophages, acidic pH can strengthen rhythms by enhancing
214 amplitude and speeding up the circadian clock, but may impair ability to maintain synchrony. Notably,
215 changes in amplitude and period occurred in a dose-dependent fashion as pH decreased, indicating that
216 rhythms are altered in a pH-dependent manner. In contrast, pro-inflammatory macrophages cultured at
217 pH 6.5 exhibited suppressed amplitude, elongated period, and decreased damping rate of rhythms
218 compared to those cultured at pH 7.4 (Figure 2C; Supplementary Figure 4A). This suggests that in pro-
219 inflammatory macrophages, acidic pH can weaken rhythms by decreasing amplitude and slowing down
220 the speed of the clock, but may promote the ability to maintain synchrony. Low pH was also observed to
221 alter the expression of the circadian clock genes *Per2*, *Cry1*, and *Nr1d1* (REV-ERBα) over time across
222 different macrophage phenotypes, confirming that multiple components of the circadian clock are
223 altered by acidic pH (Figure 2D-F). Notably, the patterns in expression of circadian genes did not always

224 match the patterns of PER2-Luc levels observed by LumiCycle. This is perhaps unsurprising, as circadian
225 rhythms are regulated at multiple levels (transcriptional, post-transcriptional, translational, post-
226 translational); as a result, circadian patterns observed in circadian proteins such as PER2-Luc do not
227 always match those of their gene transcripts[77]. Together, these data indicate that exposure to acidic
228 pH can induce changes in circadian rhythms of macrophages. Interestingly, our data indicate that while
229 rhythms of unstimulated and pro-resolution macrophages are enhanced under acidic pH despite
230 increased damping rate, rhythms of pro-inflammatory macrophages are suppressed under acidic
231 conditions but have improved damping rate. This suggests that acidic pH modulates rhythms differently
232 in macrophage of different phenotypes.
233
234 The observation that acidic pH can enhance rhythms is particularly interesting, given that acidic pH is a
235 stressful condition that can compromise macrophage survival (Supplementary Figure 4B)[30]. In line with
236 their documented enhanced glycolytic capacity, pro-inflammatory macrophages acidified the media over
237 time (Supplementary Figure 4C). Notably, while pH of the media the pro-inflammatory macrophages
238 were cultured in decreased over time pH, the pH differential between the pH 7.4, pH 6.8, and pH 6.5
239 samples groups of pro-inflammatory macrophages was maintained out to 2 days, consistent with the
240 changes in rhythms that we observe and measure between these groups.
241
242 While BMDMs are a widely used model for studying macrophages *in vitro*, there are biological
243 differences between BMDMs generated in culture and tissue-resident macrophages. Thus, we sought to
244 determine whether our observations of pH-induced changes in rhythms were relevant to tissue-resident
245 macrophages differentiated *in vivo*. To this end, we harvested peritoneal macrophages from mice
246 expressing PER2-Luc in the morning at ZT0 (6 AM) or in the evening at ZT12 (6 PM). Peritoneal
247 macrophages were cultured in media at neutral pH of 7.4 or acidic pH of 6.5 and observed by LumiCycle.

248 Recapitulating our results in BMDMs, peritoneal macrophages exhibited increased amplitude, decreased
249 period, and increase rate of damping at pH 6.5 compared to pH 7.4 (Figure 3A). To test whether pH-
250 driven changes in circadian rhythms of peritoneal macrophages were reflected at the mRNA level, we
251 compared expression of circadian clock genes in peritoneal macrophages cultured at neutral pH 7.4 or
252 acidic pH 6.8 for 24 hours using publicly available RNA-sequencing data [30]. In line with altered
253 circadian rhythms observed by Lumicycle, peritoneal macrophages cultured at pH 6.8 expressed different
254 levels of circadian clock genes than peritoneal macrophages culture at pH 7.4 (Figure 3B). The trends in
255 changes of gene expression in peritoneal macrophages cultured at pH 6.8 matched what we observed in
256 BMDMs, where low pH generally led to higher levels of circadian clock gene expression (Figure 2D-F).
257 These data support our observations by LumiCycle and indicate that acidic pH drives transcriptional
258 changes in multiple components of the circadian clock. In all, these data are evidence that pH-dependent
259 changes in circadian rhythms are relevant to *in vivo*-differentiated macrophages.
260
261 Circadian rhythms confer time-of-day variability in response to stimuli. As we have observed that acidic
262 pH can influence circadian rhythms of peritoneal macrophages, we sought to understand if peritoneal
263 macrophages would be more or less susceptible to pH-induced changes in rhythms depending on time of
264 day of exposure. To this end, we compared the magnitude of change in amplitude, period, and damping
265 in peritoneal macrophages when exposed to acidic pH 6.5 compared to neutral pH 7.4 at different times
266 of day (Figure 3C). We observed no significant difference in the pH-driven change in amplitude, period,
267 or damping in rhythms of peritoneal macrophages taken in the morning at ZT0 compared to those taken
268 in the evening at ZT12. This indicates that the influence of pH on rhythms of macrophages was similar
269 when exposed to acidic pH in the morning or in the evening, which suggests that macrophages are
270 similarly susceptible to pH-induced changes in rhythms regardless of time of day of exposure.
271

272 **Lactate alters circadian rhythms of macrophages in a manner distinct from acidic pH.**

273

274 Elevated lactate concentrations often co-localize to regions of high acidity, due to the export of both
275 protons and lactate by glycolytic cells[89-91]. In tumors, concentration of lactate has been observed to
276 be present in concentrations of up to 30mM, which are elevated over typical lactate levels in blood and
277 healthy tissue of 1.5-3mM[92]. There are previous reports that lactic acid can promote polarization of
278 macrophages toward a pro-resolution phenotype[93]. Thus, we sought to understand if lactate may be a
279 feature of the TME capable of influencing circadian rhythms of macrophages, in addition to acidic pH. To
280 this end, we cultured BMDMs in the presence or absence of 25 mM sodium-L-lactate. In line with
281 previous observations, BMDMs exposed to lactate had elevated levels of *Vegf*; however, we did not
282 observe significant elevation of *Arg1* (Figure 4A)[93].

283

284 We next cultured BMDMs at normal pH 7.4 or acidic pH 6.5, in the presence or absence of 25 mM
285 sodium-L-lactate, and monitored circadian rhythms (Figure 4B,C). Rhythms of BMDMs at pH 7.4 exposed
286 to lactate had an elongated period and decreased damping time compared to BMDMs cultured at pH 7.4
287 without lactate (Figure 4B). This suggests that lactate can slow the circadian clock and may impair the
288 ability of macrophages to maintain synchrony. Interestingly, these changes in rhythms are different from
289 those observed in acidic conditions, indicating that lactate can modulate circadian rhythms in
290 macrophages in a manner distinct from acidic pH.

291

292 As previously observed, macrophages exposed to acidic pH 6.5 exhibited increased amplitude, shortened
293 period, and increased damping rate of circadian rhythms. When BMDMs were exposed to both acidic pH
294 and elevated lactate, the increased amplitude observed at pH 6.5 is maintained; however, the shortened
295 period observed at pH 6.5 is lost, with period lengthened in BMDMs cultured in 25 mM sodium-l-lactate.

296 The increased damping rate of rhythms in BMDMs cultured at pH 6.5 compared to pH 7.4 is maintained,
297 and is further dampened by exposure to lactate. These data indicate that changes in rhythms associated
298 with acidic conditions persisted when co-exposed to elevated lactate. Lactate was also observed to alter
299 expression of the circadian clock genes *Per2*, *Cry1*, and *Nr1d1* over time in BMDMs cultured at pH 6.5,
300 while having more subtle effects at pH 7.4 (Figure 4C). Notably, lactate blunted the effect of pH 6.5 on
301 *Cry1* expression, while enhancing the effect of low pH on *Nr1d1* expression. In all, these data indicate
302 that concentration of lactate similar to that present in the TME can influence circadian rhythms and
303 circadian clock gene expression of macrophages. Lactate altered rhythms differently than acidic pH, and
304 when macrophages were exposed to acidic pH and lactate together, rhythms were further altered. This
305 suggests that when macrophages are exposed to multiple conditions capable of altering circadian
306 rhythms, each condition may contribute to a combined effect on rhythms that differs from its individual
307 impact.
308
309 **Cancer cell supernatant alters circadian rhythms in macrophages in a manner partially reversed by**
310 **neutralization of pH.**
311
312 We have observed that polarizing stimuli, acidic pH, and lactate can alter circadian rhythms. However,
313 the tumor microenvironment is complex. Cancer cells secrete a variety of factors and deplete nutrients
314 in the environment. To model this, we cultured BMDMs in RPMI or supernatant collected from KCKO
315 cells, which are a murine model of pancreatic ductal adenocarcinoma (PDAC)[94, 95], at pH 6.5 or
316 neutralized to pH 7.4 (Supplementary Figure 5). Circadian rhythms of BMDMs cultured in cancer cell
317 supernatant at pH 7.4 or pH 6.5 exhibited increased amplitude and lengthened period compared to
318 RPMI control at pH 7.4 or 6.5, respectively, indicating that cancer cell supernatant contains factors that
319 can alter circadian rhythms of BMDMs. Notably, BMDMs cultured in cancer cell supernatant at pH 6.5

320 had increased amplitude and shortened period compared to BMDMs cultured in cancer cell-conditioned
321 media at pH7.4, indicating that pH-driven changes in rhythms were maintained in BMDMs cultured in
322 cancer cell supernatant. When the pH of cancer cell supernatant was neutralized to pH7.4, the increased
323 amplitude was decreased, and the shortened period was lengthened, indicating that neutralizing acidic
324 pH partially reverses the changes in rhythms observed in macrophages cultured in cancer cell
325 supernatant at pH 6.5. These data further support our observations that acidic pH can alter circadian
326 rhythms of macrophages both alone and in combination with various factors in the TME.
327
328 **Induction of cAMP signaling alone is not sufficient to fully drive changes in circadian rhythms**
329 **associated with acidic pH.**
330
331 Evidence in the literature suggests that acidic pH is primarily sensed by macrophages via certain G
332 protein-coupled receptors (GPCRs), inducing an increase in intracellular cAMP that drives downstream
333 signaling through the cAMP pathway[29]. Transcriptional changes downstream of cAMP signaling
334 subsequently promote a pro-resolution phenotype[29, 96, 97]. Transcription of the *Crem* isoform *Icer* is
335 also induced downstream of cAMP signaling, and has been used as a "biomarker" for macrophages
336 exposed to acidic conditions in tumors[29]. In line with previous reports, we have observed induction of
337 *Icer* in macrophages under acidic pH (Supplementary Figure 3B), suggesting that cAMP signaling is being
338 induced under acidic conditions [29]. This occurs as early as 2 hours, concurrent with changes in
339 rhythms, which are observed by 6 hours following exposure to acidic conditions. It has been shown that
340 induction of cAMP signaling alone is sufficient to drive a pro-resolution phenotype in macrophages
341 similar to that observed under acidic conditions[29, 96]. Additionally, cAMP signaling has been
342 previously observed to modulate circadian rhythms in SCN and rat fibroblasts[98, 99]. Thus, we sought to

343 understand if the cAMP signaling pathway may be mediating the pH-induced changes in circadian
344 rhythms in macrophages.
345
346 The synchronization protocol we use to study circadian rhythms in BMDMs involves a 24-hour period of
347 serum starvation followed by 2 hours of serum shock. It has previously been shown that serum shock
348 can induce signaling through the cAMP pathway in rat fibroblasts[98]. To determine whether the
349 synchronization protocol impacts cAMP signaling in macrophages, we harvested macrophages before
350 and after serum shock. We then assessed *Icer* expression and phosphorylation of cyclic AMP-response
351 element binding protein (CREB), which occur downstream of cAMP and have been used as readouts to
352 assess induction of cAMP signaling in macrophages[29, 96, 100]. Serum shock of macrophages following
353 serum starvation led to rapid phosphorylation of CREB and *Icer* expression that quickly returned to
354 baseline (Supplementary Figure 2D,E). This indicates that serum starvation followed by serum shock in
355 the synchronization protocol we use to study circadian rhythms in BMDMs induces transient signaling
356 through the cAMP signaling pathway.
357
358 As acidic pH induces signaling through the cAMP pathway, we sought to determine whether acidic pH
359 independently contributed to the pH-driven changes in circadian rhythms we observe in BMDMs. To test
360 this, we omitted the synchronization step and observed BMDM rhythms by LumiCycle when cultured in
361 neutral pH 7.4 or acidic pH 6.8 or pH 6.5 (Supplementary Figure 6). Circadian rhythms of BMDMs
362 cultured at pH 6.5 exhibited similar changes as previously observed, with enhanced amplitude and
363 shortened period relative to BMDMs at pH 7.4. This indicates pH-driven changes observed in circadian
364 rhythms of BMDMs occur in the absence of prior serum starvation and serum shock.
365

366 To determine if elevation in intracellular cAMP alone was sufficient to drive changes in rhythms observed
367 in macrophages under acidic conditions, we treated macrophages with forskolin, an adenylyl cyclase
368 activator that stimulates production of cAMP, or 3-isobutyl-1-methylxanthine (IBMX), which drives
369 accumulation of cAMP through inhibition of phosphodiesterases (PDEs). We used a range of doses
370 similar to those previously shown to induce cAMP signaling in macrophages in the literature[29, 98,
371 100]. Treatment with either forskolin or IBMX increased amplitude of rhythms in macrophages, but not
372 to the same magnitude as acidic pH, and did not result in a changed period (Figure 5A,B). Moreover,
373 amplitude of rhythms was not altered in forskolin- or IBMX-treated macrophages at pH 6.5, indicating
374 that neither forskolin nor IBMX had any additional effect on rhythms under acidic conditions. These data
375 indicate that in macrophages, cAMP signaling alone induces enhanced amplitude of rhythms similar to
376 low pH, but the magnitude of this change is far less; additionally, period, which is altered under acidic
377 conditions, remains unchanged. This suggests that cAMP signaling may contribute to but is not sufficient
378 to fully recapitulate the changes in rhythms observed under acidic conditions.
379
380 **Adenylyl cyclase inhibitor MDL-12330A suppresses pH-mediated changes in amplitude of circadian**
381 **rhythms and pro-resolution phenotype without suppressing cAMP signaling.**
382
383 To further test whether pH-induced changes in rhythms are mediated by cAMP signaling, we treated
384 BMDMs with MDL-12330A (henceforth referred to as MDL-12), an adenylyl cyclase inhibitor which has
385 previously been shown to suppress cAMP signaling in macrophages under acidic conditions[29]. When
386 BMDMs cultured at pH 6.5 were treated with MDL-12, the elevated amplitude of rhythms observed at
387 pH 6.5 was suppressed (Figure 5C). Notably, this occurred in a dose-dependent manner, suggesting that
388 this is a drug-dependent effect. Importantly, rhythms of MDL-12-treated macrophages at pH 7.4 had
389 similar amplitude to vehicle-treated macrophages at pH 7.4. This suggests that the inhibitory effect of

390 MDL-12 on pH-induced enhancement of amplitude in macrophage rhythms was specific to acidic
391 conditions. However, MDL-12 treatment of macrophages at pH 7.4 resulted in shortened period and
392 decreased damping rate compared to vehicle-treated macrophages. Together, MDL-12-mediated
393 suppression of pH-driven changes in amplitude, but not period or damping, suggests that the pH-driven
394 changes in these different parameters of rhythms may occur through different pathways. Interestingly,
395 although the adenylyl cyclase inhibition by MDL-12 is reported to be irreversible, we found that
396 pretreatment up to 2 hours was not sufficient to suppress pH-induced changes in amplitude
397 (Supplementary Figure 7). Only when macrophages continued to be cultured with MDL-12 while exposed
398 to acidic conditions was amplitude suppressed. Meanwhile, co-treating cells with acidic pH and MDL12
399 without any pre-treatment was sufficient to suppress elevation of amplitude under acidic conditions
400 (Figure 5C).
401
402 Evidence suggests that acidic pH signals through the cAMP pathway to promote a pro-resolution
403 phenotype in macrophages, with induction of *Icer* occurring directly downstream of cAMP signaling[29].
404 Despite preventing changes in amplitude under acidic pH, MDL12 treatment at the dose and treatment
405 schedule used does not suppress induction of *Icer* in macrophages under acidic conditions (Figure 5D).
406 However, induction of *Arg1* expression in macrophages under acidic conditions was suppressed by MDL-
407 12. This suggests that at the dose and treatment strategy used, MDL-12 partially suppresses the
408 response of macrophages to acidic pH by suppressing the pH-driven polarization toward a pro-resolution
409 phenotype and changes in amplitude.
410
411 To further investigate how MDL-12 was influencing cAMP signaling at the dose and treatment strategy
412 used, we evaluated phosphorylation of cyclic AMP-response element binding protein (CREB).
413 Phosphorylation of CREB occurs downstream of cAMP and has commonly been used as a readout to

414 assess induction of cAMP production in macrophages[96, 100]. In line with evidence in the literature
415 that exposure to acidic pH drives an increase in intracellular cAMP in macrophages[29], we observed
416 that downstream phosphorylation of CREB was elevated in macrophages exposed to acidic pH compared
417 to those in non-acidic conditions (Figure 5E,F). Unexpectedly, pCREB levels remained elevated in BMDMs
418 at pH 6.5 despite treatment with MDL-12, indicating that pH-driven phosphorylation of CREB was not
419 suppressed by MDL12 treatment. In fact, pCREB was elevated in MDL-12-treated BMDMS at pH 7.4,
420 suggesting that MDL-12 treatment alone induced phosphorylation of CREB. This is particularly surprising
421 considering that amplitude was not altered in MDL-12-treated macrophages at neutral pH 7.4 despite
422 elevated pCREB. This suggests that some elements of the cAMP signaling pathway, such as pCREB, may
423 be divorced from the pH-induced changes in rhythms. Collectively, our data indicate that while the cAMP
424 signaling pathway is induced under acidic conditions, pH-induced changes in rhythms may not be
425 attributed to cAMP signaling alone, as MDL-12 treatment suppressed pH-induced changes in amplitude
426 of rhythms, but not period or damping, without suppressing signaling through the cAMP pathway.
427
428 **There is evidence of circadian disorder in the tumor-associated macrophage population.**
429
430 As we have observed that acidic pH at levels commonly observed in the TME can alter circadian rhythms
431 in macrophages *in vitro* and *ex vivo*, we next sought to investigate whether circadian rhythms can be
432 altered in the TME *in vivo*. Using publicly available data, we analyzed gene expression of tumor-
433 associated macrophages (TAMs) isolated from LLC (Lewis Lung carcinoma) tumors in mice [101]. As a
434 positive control for circadian clock disruption, we used data from BMAL1 KO peritoneal macrophages
435 [44]. BMAL1 KO macrophages have a genetic disruption of the circadian clock due to the loss of Bmal1,
436 the central clock gene. As a result, circadian rhythms of BMAL1 KO macrophages are disrupted, lacking
437 rhythmicity and downstream circadian regulation of macrophage function (Supplementary Figure 8)[45,

438 54]. In line with previous observations, TAMs had elevated expression of *Arg1* relative to WT and BMAL1
439 KO peritoneal macrophages (Figure 6A). Expression of *Crem*, which encodes *Icer*, was also elevated in
440 TAMs, indicating that these TAMs were exposed to acidic conditions within the TME (Figure 6A)[29].
441
442 To understand the status of the circadian clock in TAMs, we performed clock correlation distance (CCD)
443 analysis. This analysis has previously been used to assess functionality of the circadian clock in whole
444 tumor and in normal tissue[102]. As the circadian clock is comprised of a series of
445 transcription/translation feedback loops, gene expression is highly organized in a functional, intact clock,
446 with core clock genes existing in levels relative to each other irrespective of the time of day. In a
447 synchronized population of cells, this ordered relationship is maintained at the population level, which
448 can be visualized in a heatmap. CCD is designed to compare circadian clock gene co-expression patterns
449 between different tissues and cell types. To accomplish this, CCD was built using datasets from multiple
450 different healthy tissues from mouse and human to be a universal tool to compare circadian rhythms.
451 Each sample is compared to a reference control built from these multiple tissues (Figure 6B)[102]. To
452 validate the use of this analysis for assessing circadian disorder in macrophages, we performed CCD
453 analysis using publicly available RNA-sequencing data from bone marrow-derived macrophages and wild
454 type peritoneal macrophages, as a healthy control for functional rhythms in a synchronized cell
455 population, and BMAL1 KO peritoneal macrophages, as a positive control for circadian disorder[44]. We
456 found that gene co-expression of clock genes was ordered in wild type macrophages with functional
457 clocks and intact circadian rhythms (Figure 6C, Supplementary Figure 8). In contrast, clock gene co-
458 expression is disordered in BMAL1 KO macrophages with a genetic disruption of the circadian clock,
459 leading to disruption of circadian rhythms (Figure 6C,D, Supplementary Figure 8). This indicates that CCD
460 analysis can be used to measure circadian disorder in a macrophage population. To assess the status of
461 the circadian clock in tumor-associated macrophages, we next performed CCD analysis using RNA-

462 sequencing data of TAMs derived from LLC tumors[101]. Clock correlation distance analysis revealed
463 that, similar to the BMAL1 KO peritoneal macrophages, the co-expression relationship between the core
464 circadian clock genes in TAMs is significantly more disordered than that of WT peritoneal macrophages
465 (Figure 6C,D). Weighted gene co-expression network analysis (WGCNA) has been used as an alternate
466 approach to measure the co-variance between clock genes and thus assess bi-directional correlations
467 among the core clock gene network in healthy tissue and tumor samples [103]. In line with the circadian
468 disorder observed by CCD, while many bi-directional correlations among the core clock gene network
469 were significant and apparent in wild type peritoneal macrophages, these relationships were altered or
470 abolished within BMAL1 KO peritoneal macrophages and TAM samples, and in some cases replaced by
471 new relationships (Figure 6E). This indicates that there is population-level disorder in the circadian
472 rhythms of tumor-associated macrophages in murine lung cancer.
473
474 We next assessed the status of the circadian clock in human TAMs from NSCLC patients. We performed
475 CCD with publicly available RNA-seq data of tumor-adjacent macrophages and tumor-associated
476 macrophages from NSCLC patients, using alveolar macrophages from healthy donors as a control[104,
477 105]. To assess the contribution of the acidic TME to circadian disorder, we subset TAM NSCLC patient
478 samples into groups (*Crem* high TAMs and *Crem* low TAMs) based on median *Crem* expression. Notably,
479 in macrophages from human NSCLC there was a trend toward disorder in *Crem* low but not *Crem* high
480 TAM samples (Figure 7A,B). Additionally, the co-variance among core clock genes observed in alveolar
481 macrophages from healthy donors was absent within *Crem* low and *Crem* high TAM samples (Figure 7C).
482 In all, these data indicate that there is population-level disorder in the circadian rhythms of tumor-
483 associated macrophages in humans and mice, suggesting that circadian rhythms are indeed altered in
484 macrophages within the TME.
485

486 **Heterogeneity of circadian rhythms within a population can underlie circadian disorder as measured**
487 **by CCD.**
488
489 Circadian disorder assessed by CCD has previously been used to infer disruption of circadian
490 rhythms[106]. Indeed, we observed that genetic disruption of circadian rhythms by BMAL1 KO resulted
491 in a disordered clock, as observed in peritoneal macrophages (Figure 6B). However, since CCD is a
492 population-level analysis, heterogeneity of rhythms, as observed in a desynchronous cell population,
493 rather than disruption of rhythms, may also underlie the circadian disorder observed by CCD.
494 Heterogeneity in macrophage phenotype, exposure to acidic pH, and lactate are all factors present in the
495 TME and relevant to tumor-associated macrophages. We have observed that each of these factors can
496 alter circadian rhythms in macrophages, both alone and in combination with each other. Furthermore,
497 we have observed a trend toward circadian disorder in *Crem* low TAM samples but not *Crem* high TAM
498 samples. Thus, we sought to understand if heterogeneity in macrophage rhythms could be contributing
499 to the disorder in clock gene co-expression and poor CCD score indicative of population-level disorder in
500 TAM rhythms.
501
502 To address this, we examined if differences in rhythms of macrophages within a population might
503 contribute to population-level disorder as measured by CCD. To this end, we used publicly available data
504 of peritoneal macrophages taken at different times of day in four-hour intervals across two days[36]. We
505 then constructed four different sample groups in which samples were pooled according to time of day of
506 harvest. As a control for a synchronized cell population with homogenous rhythms, samples taken at the
507 same time of day were pooled. We then modeled a progressively desynchronized population with
508 increased differences in phase of rhythms by pooling samples that were taken four hours apart, eight
509 hours apart, or twelve hours apart (Figure 8A). CCD was then performed on these four populations

510 (Figure 8B). CCD score worsened as populations became increasingly desynchronized, with the 12hr
511 desynchronized population having a significantly worse CCD score than synchronized, homogenous
512 macrophage population (Figure 8C). This indicates that as circadian rhythms of individual macrophages
513 within a population become more different from each other, circadian disorder increases at the
514 population-level. This is further supported by WGCNA, which revealed that the significant co-variance of
515 circadian clock genes in the synchronized population was progressively altered and lost as the population
516 is increasing desynchronized to 12 hours (Supplementary Figure 9). The results of these analyses
517 suggests that heterogeneity in rhythms, as observed with desynchrony, may underlie population-level
518 disorder of the circadian clock as measured by CCD.
519
520 **Tumor-associated macrophages exhibit heterogeneity in circadian clock gene expression.**
521
522 Our findings suggested that heterogeneity of the circadian clock may lead to disorder in bulk
523 macrophage populations, but did not reveal if specific gene expression changes exist in tumor-associated
524 macrophages at the single-cell level. To determine whether heterogeneity exists within the expression of
525 circadian clock genes of the tumor-associated macrophage population, we analyzed publicly available
526 single-cell RNA sequencing data of macrophages isolated from B16-F10 tumors[107]. To capture the
527 heterogeneity of macrophage subsets within the TAM population, we performed unbiased clustering
528 (Figure 9A). We then performed differential gene expression to determine if circadian clock genes were
529 differentially expressed within the TAM subpopulations. The circadian clock genes *Bhlhe40* (DEC1),
530 *Bhlhe41* (DEC2), *Nfil3* (E4BP4), *Rora* (RORα), *Dbp* (DBP), and *Nr1d2* (REV-ERBβ) were significantly
531 (adj.p<0.005) differentially expressed between TAM clusters (Figure 9B). This indicates that there is
532 heterogeneity in expression of circadian clock genes within the TAM population.
533

534 We next sought to determine whether differences in circadian clock gene expression between TAM
535 subpopulations were associated with exposure to acidic pH in the TME. To this end, we first assessed
536 *Crem* expression in the TAM subpopulations that were identified by unbiased clustering. *Crem* expression
537 was significantly higher in TAM clusters 4, 5, and 6 compared to TAM clusters 1-3 and 7-9 (Figure 9C).
538 Clusters were subset based on *Crem* expression into *Crem* high (clusters 4-6) and *Crem* low (clusters 1-3,
539 7-9) (Figure 9D), and differential gene expression analysis was performed. The circadian clock genes
540 *Nfil3, Rora, Bhlhe40,* and *Cry1* (CRY1) were significantly (adj.p<0.005) differentially expressed between
541 *Crem* high and *Crem* low TAMs (Figure 9E). This suggests that acidity within the TME is associated with
542 heterogeneity in expression of circadian clock genes within the TAM population. Interestingly, expression
543 of circadian clock genes varied between clusters designated as *Crem* high or *Crem* low (Figure 9B); for
544 instance, *Nfil3* was more highly expressed in cluster 1 than cluster 3, both of which had low *Crem*
545 expression. This indicates that there is diversity in circadian clock gene expression within the *Crem* high
546 and *Crem* low groups, suggesting that acidic pH is not the only factor in the TME that can alter the
547 circadian clock. Collectively, these data suggest that there is heterogeneity in the circadian clock of
548 macrophages within the TAM population that is driven in part by acidic pH.
549
550 **Circadian rhythms of macrophages can influence tumor growth in a murine model of pancreatic**
551 **cancer.**
552
553 We next sought to determine how circadian rhythms in tumor-associated macrophages may influence
554 tumor growth in KCKO, a murine model of PDAC [94, 95]. To this end, we used a genetic disruption of the
555 circadian clock in macrophages. Myeloid-specific genetic mouse models are not macrophage-specific, so
556 co-injection experiments are commonly used to determine macrophage-specific roles[93, 108-110].
557 Thus, we co-injected BMDMs from WT or BMAL1 KO mice along with KCKO cells into WT mice, and

558 tumor growth was measured. We saw a significant increase in the growth of tumors co-injected with
559 BMAL1 KO macrophages compared to those co-injected with WT macrophages (Figure 10). These results
560 suggest intact circadian rhythms of macrophages can restrain tumor growth, in agreement with similar
561 published findings in a murine model of melanoma[109].
562

563 ## Discussion

564

565 Macrophages experience altered environmental conditions within the tumor microenvironment, but
566 how these may affect macrophage circadian rhythms remains unclear. Here we assessed whether
567 circadian rhythms are altered in macrophages within the TME. To this end, we investigated whether
568 conditions commonly associated with the tumor microenvironment could influence circadian rhythms in
569 macrophages. As TAMs are phenotypically heterogenous, we first assessed circadian rhythms in
570 macrophages polarized toward different phenotypes. We found that polarization state affected circadian
571 rhythmicity, with pro-inflammatory macrophages exhibiting far weaker rhythms that pro-resolution
572 macrophages (Figure 1). We then modeled acidic conditions in the TME by exposing macrophages to pH
573 and lactate levels similar to those found in the TME, and found that low pH in particular dramatically
574 altered the rhythms of macrophages (Figures 2-4). Changes in cAMP signaling may contribute to these
575 changes in rhythmicity, but low pH induced alterations far beyond what is observed by enhancing cAMP
576 signaling pharmacologically (Figure 5A,B). While the adenylyl-cyclase inhibitor MDL-12 largely rescued
577 the changes in amplitude observed in low pH, our data suggest that a pathway other than canonical
578 cAMP signaling may be involved in this effect (Figure 5C-F). Finally, we assessed the status of the
579 circadian clock in tumor-associated macrophages, the potential contribution of heterogeneity in
580 circadian rhythms to population-level rhythms, and assessed whether the circadian regulation of
581 macrophages impacts tumor growth. Our results indicated that macrophage rhythms are disordered

582 within tumors (Figure 6,7), and that heterogeneity in rhythms within the tumor-associated macrophage
583 population may underlie this observed circadian disorder (Figure 8), which was supported by our
584 observations of heterogeneity in circadian clock gene expression within the TAM population from scRNA-
585 seq data (Figure 9). We further demonstrated that the intact macrophage circadian clock can suppress
586 tumor growth (Figure 10). Overall, our results for the first time demonstrate that exposure of
587 macrophages to conditions associated with the tumor microenvironment can influence circadian
588 rhythms, a key aspect of macrophage biology.
589
590 A critical question in understanding the role of circadian rhythms in macrophage biology is determining
591 how different polarization states of macrophages affect their internal circadian rhythms. This is especially
592 important considering that tumor-associated macrophages are a highly heterogeneous population. Our
593 data indicate that compared to unstimulated macrophages, rhythms are enhanced in pro-resolution
594 macrophages, characterized by increased amplitude and improved ability to maintain synchrony; in
595 contrast, rhythms are suppressed in pro-inflammatory macrophages, characterized by decreased
596 amplitude and impaired ability to maintain synchrony (Figure 1). These agree with previously published
597 work showing that polarizing stimuli alone and in combination with each other can alter rhythms
598 differently in macrophages[80, 81]. In a tumor, macrophages exist along a continuum of polarization
599 states and phenotypes[18-21, 24]. Thus, while our characterizations of rhythms in *in vitro*-polarized
600 macrophages provide a foundation for understanding how phenotype affects circadian rhythms of
601 macrophages, further experiments will be needed to assess macrophages across the full spectrum of
602 phenotypes. Indeed, alteration of rhythms may be just as highly variable and context-dependent as
603 phenotype itself.
604

605 In addition to polarizing stimuli, tumor-associated macrophages are exposed to a variety of conditions
606 within the tumor microenvironment that may alter their circadian rhythms. We observed that exposure
607 to acidic pH altered rhythms in macrophages, increasing amplitude of pro-resolution macrophages but
608 suppressing amplitude of pro-inflammatory macrophages (Figure 2). This indicates that pH affects
609 rhythms differently depending on phenotype, hinting at additional layers of complexity in how the
610 environment could contribute to changes in circadian rhythms. Even further changes in rhythms were
611 observed when macrophages were exposed to lactate in conjunction with acidic pH (Figure 4). These
612 observations suggest that the combination of stimuli present in the microenvironment such as lactate
613 and low pH, as well as various polarizing stimuli, can each contribute to modulate rhythms, resulting in
614 highly context-dependent changes in circadian rhythms of macrophages based on the
615 microenvironment. As macrophages are highly plastic and exquisitely capable of sensing and responding
616 to their environment, one could reason that changes in circadian rhythms, and downstream circadian
617 regulation, are a mechanism by which macrophages can adopt different programs to respond to their
618 environment.
619
620 Elucidating the role of circadian rhythms in regulation of macrophage biology necessitates a better
621 understanding of the crosstalk between phenotype and circadian rhythms. Although lactate polarizes
622 macrophages toward a pro-resolution phenotype similar to acidic pH[30, 93], exposure to lactate had
623 different effects on circadian rhythms – and in some cases, circadian clock gene expression – than
624 exposure to acidic pH (Figure 4). Sensing of lactate occurs through different pathways than acid-sensing,
625 which may contribute to the different ways in which these two stimuli modulate circadian rhythms of
626 macrophages[111]. One previously published finding that may offer mechanistic insight into how
627 phenotype can influence circadian rhythms is the suppression of Bmal1 by LPS-inducible miR-155[54]. It
628 has also been observed that RORα-mediated activation of Bmal1 transcription is enhanced by PPARγ co-

629 activation[112]. In macrophages, PPARγ expression is induced upon stimulation with IL-4 and plays a key
630 role in alternative activation of macrophages, promoting a pro-resolution macrophage phenotype, and
631 supporting resolution of inflammation[113-115]. Such observations prompt the question of whether
632 there are yet-unidentified factors induced downstream of various polarizing stimuli that can modulate
633 expression of circadian genes at the transcriptional and protein levels. Further work is required to
634 understand the interplay between macrophage phenotype and circadian rhythms.
635
636 It was previously observed that acidic pH can disrupt circadian rhythms in cell lines[32]. However, while
637 acidic pH altered rhythms in macrophages, it did not ablate them. This suggests that the influence of
638 acidic pH on circadian rhythms can vary between cell types. pH-induced circadian disruption was found
639 to be driven by inhibition of mTORC1 activity in cell lines, and there was evidence to suggest that
640 mTORC1 activity was sensitive to pH in T cells [116]. Thus, the role of mTORC1 activity in mediating pH-
641 driven changes in circadian rhythms of macrophages will be a topic of future investigation.
642
643 The mechanism through which acidic pH can modulate the circadian clock in macrophages remains
644 unclear. Evidence in the literature suggests that acidic pH promotes a pro-resolution phenotype in
645 macrophages by driving signaling through the cAMP pathway[29]. It has previously been shown that
646 cAMP signaling can modulate the circadian clock[99]. However, our data indicated that cAMP signaling
647 was not fully sufficient to confer pH-mediated changes in circadian rhythms of macrophages (Figure
648 5A,B). Treatment with MDL-12, commonly known as an inhibitor of adenylyl cyclase[29, 117], resulted in
649 suppression of pH-induced changes in amplitude of circadian rhythms but did not inhibit signaling
650 through the cAMP signaling pathway (Figure 5C,D). While MDL-12 is commonly used as an adenylyl
651 cyclase inhibitor, it has also been documented to have inhibitory activity toward phosphodiesterases
652 (PDEs) and the import of calcium into the cytosol through various mechanisms[118, 119]. This is of

653 particular interest, as calcium signaling has also been shown to be capable of modulating the circadian
654 clock[120]. Furthermore, while acid-sensing through GPCRs have been the most well-characterized
655 pathways in macrophages, there remain additional ways in which acidic pH can be sensed by
656 macrophages such as acid-sensing ion channels[121, 122]. Further work is required to understand the
657 signaling pathways through which pH can influence macrophage phenotype and circadian rhythms.
658
659 We observed that acidic pH appears to enhance circadian rhythms of unstimulated and pro-resolution
660 macrophages, and we and others have shown evidence that macrophages are exposed to an acidic
661 environment within the TME[28, 29]. Interestingly, analysis of TAMs by clock correlation distance (CCD)
662 presents evidence that rhythms are disordered in bulk TAMs compared to other macrophage
663 populations (Figure 6). CCD is one of the most practical tools currently available to assess circadian
664 rhythms due to its ability to assess rhythms independent of time of day and without the need for a
665 circadian time series, which is often not available in publicly available data from mice and humans[102].
666 However, CCD is limited in that it is a measure of population-level circadian rhythms. Our data indicate
667 that heterogeneity of circadian rhythms within a given population can underlie circadian disorder
668 observed by CCD (Figure 8). Indeed, we observed differences in the circadian clock of *Crem* low human
669 TAM samples compared to *Crem* high human TAM samples, suggesting that acidic pH influences
670 circadian disorder in TAMs (Figure 7). Interestingly, *Crem* low TAM samples exhibited a trend toward
671 disorder while *Crem* high TAM samples did not. This is of particular interest, as we have observed that
672 acidic pH can enhance circadian rhythms in macrophages, raising the question of whether acidic pH
673 promotes or protects against circadian disorder. We have shown that various stimuli can alter rhythms of
674 macrophages in a complex and contributing manner, including polarizing stimuli, acidic pH, and lactate.
675 TGFβ is produced by a variety of cells within the TME, and was recently identified as a signal that can
676 modulate circadian rhythms[123, 124]. Additionally, when we exposed macrophages to cancer cell-

677 conditioned media, rhythms were modulated in a manner distinct from acidic pH or lactate, with these
678 changes in rhythms partially reversed by neutralization of the cancer cell-conditioned media pH
679 (Supplementary Figure 5). It is conceivable that, in addition to acidic pH, other stimuli in the TME are
680 influencing circadian rhythms to drive population-level disorder that we observed by CCD.
681
682 Supporting the notion that population-level disorder may exist in TAMs, we used scRNA-sequencing data
683 and found evidence of heterogeneity between the expression of circadian clock genes in different TAM
684 subpopulations (Figure 9A, B). Phenotypic heterogeneity of TAMs in various types of cancer has
685 previously been shown[20, 21, 125, 126], and we have identified distinct TAM subpopulations by
686 unbiased clustering (Figure 9A). Within those TAM subpopulations, we identified differential expression
687 of circadian clock genes encoding transcription factors that bind to different consensus sequences: DEC1
688 and DEC2 bind to E-boxes, NFIL3 and DBP binds to D-boxes, and RORα and REV-ERBβ binds to retinoic
689 acid-related orphan receptor elements (ROREs)[127, 128]. While little is known about regulation of
690 macrophages by E-box and D-box elements beyond the circadian clock, aspects of macrophage function
691 have been shown to be subject to transcriptional regulation through ROREs[129, 130]. Thus, we
692 speculate that variations in these transcription factors may exert influence on expression of genes to
693 drive diversity between TAM subpopulations. Differential expression of circadian clock genes between
694 TAM subpopulations was also associated with *Crem* expression (Figure 9C-E), suggesting that exposure of
695 TAMs to acidic pH within the TME can alter the circadian clock. However, there remained significant
696 variation in expression of circadian clock genes within the *Crem* high and *Crem* low groups (Figure 9B),
697 suggesting that acidic pH is not the only factor in the TME that can alter the circadian clock. Together,
698 these data implicate the TME in driving heterogeneity in TAM circadian rhythms just as it drives
699 heterogeneity in TAM phenotype.
700

701 Interestingly, in contrast to our observations of circadian disorder in TAMs isolated from LLC tumors
702 (Figure 6), rhythmicity in expression of circadian genes was observed in bulk TAMs isolated from B16
703 tumors[107]. This suggests that circadian rhythms of TAMs are maintained differently in different types
704 of cancer. Notably, both of these observations were at the population level. Upon separation of the B16
705 TAM population into subsets by unbiased clustering of single-cell RNA sequencing data, we measured
706 differences in expression of circadian clock genes between TAM subpopulations (Figure 9A,B). This
707 suggests that even within a rhythmic TAM population, there is heterogeneity in the circadian clock of
708 TAM subpopulations.
709
710 Considering our observations that conditions associated with the TME can alter circadian rhythms in
711 macrophages, it becomes increasingly important to understand the relevance of macrophage rhythms to
712 their function in tumors. It has been shown that acidic pH and lactate can each drive functional
713 polarization of macrophages toward a phenotype that promotes tumor growth, with acidic pH
714 modulating phagocytosis and suppressing inflammatory cytokine secretion and cytotoxicity[28, 30, 93].
715 However, how the changes in circadian rhythms of macrophages driven by these conditions contributes
716 to their altered function remains unknown. Current evidence suggests that circadian rhythms confer a
717 time-of-day-dependency on macrophage function by gating the macrophage response to inflammatory
718 stimuli based on time-of-day. As such, responses to inflammatory stimuli such as LPS or bacteria are
719 heightened during the active phase while the inflammatory response is suppressed during the inactive
720 phase. An important future direction will be to determine how changes in circadian rhythms of
721 macrophages, such as those observed under acidic pH or high lactate, influences the circadian gating of
722 their function. Data from our lab and others suggest that disruption of the macrophage-intrinsic
723 circadian clock accelerates tumor growth, indicating that circadian regulation of macrophages is tumor-
724 suppressive in models of PDAC (our work) and melanoma [109]. This agrees with complementary

725 findings that behavioral disruption of circadian rhythms in mice (through chronic jetlag) disrupts tumor
726 macrophage circadian rhythms and accelerates tumor growth[56]**.** It remains unclear whether this is
727 through the pro-tumorigenic functions of macrophages such as extracellular matrix remodeling or
728 angiogenesis, through suppression of the anti-tumor immune response, or a combination of both
729 functions. Further work will be needed to tease apart these distinctions.
730
731 Whereas much work has been done to characterize how macrophages are regulated within the TME, the
732 impact of the TME on circadian rhythms of macrophages remained elusive. Our work uncovers a novel
733 way in which conditions associated with the TME can influence macrophage biology through modulation
734 of circadian rhythms. While the majority of studies investigating the circadian regulation of macrophages
735 have been conducted studying macrophages under homeostatic conditions or in response to acute
736 inflammation[36, 38, 44, 45, 131], our work contributes to an emerging body of evidence that the tissue
737 microenvironment can influence circadian rhythms[123]. This is increasingly important when considering
738 the role of circadian rhythms in immune responses at sites of ongoing, chronic inflammation where the
739 microenvironment is altered, such as within tumors. In identifying factors within the TME that can
740 modulate circadian rhythms of macrophages and uncovering evidence of circadian disorder within
741 tumor-associated macrophages, our work lays the foundation for further studies aimed at understanding
742 how the TME can influence the function of tumor-associated macrophages through modulation of
743 circadian rhythms.
744
745 **Limitations of the Study**
746
747 Our observations of rhythms in macrophages of different phenotypes are limited by *in vitro* polarization
748 models. It is important to note that while our data suggest that pro-inflammatory macrophages have

749 suppressed rhythms and increased rate of desynchrony, it remains unclear the extent to which these
750 findings apply to the range of pro-inflammatory macrophages found *in vivo*. We use IFNγ and LPS co-
751 treatment *in vitro* to model a pro-inflammatory macrophage phenotype that is commonly referred to as
752 'M1', but under inflammatory conditions *in vivo*, macrophages are exposed to a variety of stimuli that
753 result in a spectrum of phenotypes, each highly context-dependent. The same is true for for 'M2';
754 different tissue microenvironment are different and pro-resolution macrophages exist in a spectrum.
755 Rhythms were heavily suppressed in pro-inflammatory macrophages, which makes analysis of rhythm
756 parameters in pro-inflammatory macrophages more challenging as amplitude and signal reaches limit of
757 detection. Our observations of changes in amplitude and period in pro-inflammatory macrophages
758 compared to unstimulated macrophages agrees with the literature, where these changes in rhythms
759 have been observed using LumiCycle as well as by mRNA[80, 81]. This supports the validity and
760 reproducibility of our observations despite the challenges of observing and analyzing rhythms of pro-
761 inflammatory macrophages.
762

763 # Methods

764 **Animals**

765 Mice were maintained in individually ventilated cages with bedding and nesting material in a
766 temperature-controlled, pathogen-free environment in the animal care facility at the University of
767 Rochester. All animal protocols were approved by the University of Rochester Committee of Animal
768 Resources (UCAR). All experiments were performed in compliance with the NIH- and University of
769 Rochester-approved guidelines for the use and care of animals, as well as recommendations in the Guide
770 for the Care and Use of Laboratory Animals of the National Research Council[132]. Mice were housed on
771 a 12:12 light dark cycle. In some cases, to ease timepoint collection, mice were housed under reverse
772 lighting conditions in a 12:12 dark light cycle for at least 2 weeks prior to use in experiments. Mice used

773 for experiments were between the ages of 8-14 weeks old; both male and female mice were used. Mice
774 were euthanized humanely prior to harvesting peritoneal macrophages or bone marrow.
775
776 Previously characterized mice with a myeloid-specific deletion of BMAL1 (LysM-cre$^{+/-}$Bmal1$^{flox/flox}$;
777 referred to as BMAL1 KO mice)[45] in a C57BL/6 background were generated by crossing LysM-cre
778 mice[133] with Bmal1$^{flox/flox}$ mice[134]. These mice were further crossed with PER2-Luc mice[76] to
779 generate BMAL1 KO or wild-type control mice (LysM-cre$^{-/-}$Bmal1$^{flox/flox}$; referred to as WT) expressing
780 PER2-Luc. PER2-Luc (strain #006852), LysM-cre (strain #004781), and Bmal1$^{flox/flox}$(strain #007668) mice
781 used for breeding to generate WT and BMAL1 KO mice were purchased from the Jackson Laboratory.
782
783 **Differentiation and culture of bone marrow-derived macrophages**
784 Bone marrow-derived macrophages (BMDMs) were generated from bone marrow isolated from WT
785 mice using a well-established protocol for differentiation of BMDMs over 7 days[135, 136]. In brief, bone
786 marrow cells were seeded at 200,000 cells/mL on non-tissue culture treated-plates in BMDM
787 Differentiation Media: RPMI (Corning, CAT#MT10040CV) supplemented with 20% (v/v) L929 supernatant
788 and 10% (v/v) heat-inactivated (HI) fetal bovine serum (FBS) (Cytiva, CAT#SH30396.03), supplemented
789 with 100 U/mL Penicillin-Streptomycin (Gibco, CAT# 15140122). Cells were grown at 37°C in air enriched
790 with 5% CO_2. On day 3, additional BMDM Differentiation Media was added to cells. On day 6 of the
791 differentiation protocol, BMDMs were seeded at 1.2*10^{6} cells/mL and left in BMDM Differentiation
792 Media, and kept at 37°C in air enriched with 5% CO_2. On day 7, BMDM Differentiation Media was
793 removed and BMDMs were synchronized.
794
795 To synchronize BMDMs, we adapted a recently published method[77]. Briefly, BMDMs were first serum
796 starved for 24 hours in serum-free media (RPMI, supplemented with 100 U/mL Penicillin-Streptomycin);

797 BMDMs were then subjected to serum shock by replacing serum-free media with RPMI supplemented
798 with 50% (v/V) HI horse serum (Corning, CAT#35030CV) at 37°C in air enriched with 5% CO_2. At the end
799 of this synchronization protocol, media was replaced with Atmospheric Media, which has been
800 formulated for use at atmospheric CO_2 levels and enhanced pH stability by increasing buffering capacity
801 at low pH[32]: RPMI (Corning, CAT#50-020-PC), 25mM HEPES (Gibco, CAT#15630080), 25mM PIPES
802 (Sigma, CAT#P1851), supplemented with 10% (v/v) HI FBS and 100 U/mL Penicillin-Streptomycin[32].
803 Atmospheric Media was adjusted to pH 7.4, 6.8, or 6.5 with NaOH and filter-sterilized.
804
805 BMDMs cultured in Atmospheric Media at pH 7.4, 6.8, or 6.5 were either left unstimulated or were
806 polarized toward a pro-resolution ('M2') or pro-inflammatory phenotype ('M1') by addition of 10 ng/mL
807 IL-4 (PeproTech, CAT#214-14) and 10 ng/mL IL-13 (PeproTech, CAT# 210-13), or 50 ng/mL IFNγ
808 (PeproTech, CAT#315-05) and 100 ng/mL LPS (Invitrogen, CAT#00497693), respectively. For lactate
809 experiments, sodium-L-lactate (Sigma, CAT#L7022) or vehicle was added to Atmospheric Media for 25
810 mM sodium-L-lactate or 0 mM sodium-L-lactate in Atmospheric Media. For interrogation of cAMP
811 signaling pathway, BMDMs were cultured in Atmospheric Media at pH 7.4 or 6.5 with vehicle or 5, 10, or
812 15 µM MDL-12330A (Sigma, CAT#M182). For phenocopy experiments (Figure 5), BMDMs were not
813 synchronized prior to the experiment. BMDMs were cultured in Atmospheric Media at pH 7.4 or 6.5 with
814 vehicle or 20, 40, or 80 µM IBMX (Sigma, CAT#I5879) or forskolin (Sigma, CAT#344270). For LumiCycle
815 experiments, 100mM D-luciferin was added to Atmospheric Media at 1:1000 for 100µM D-luciferin
816 (Promega, CAT#E1602). Cells cultured in Atmospheric Media were kept at 37°C in atmospheric
817 conditions, and were either monitored over time by LumiCycle or harvested for RNA or protein at the
818 time points indicated.
819
820 **Isolation and culture of peritoneal macrophages**

821 Peritoneal exudate cells were harvested from mice as previously published[137]. To isolate peritoneal
822 macrophages, peritoneal exudate cells were seeded at $1.2*10^6$ cells/mL in RPMI/10% HI FBS
823 supplemented with 100U/mL Penicillin-Streptomycin and left at 37°C for 1 hour, after which non-
824 adherent cells were rinsed off[136]. Isolation of peritoneal macrophages using this method has been
825 shown to yield a population that is over 90% in purity[138, 139]. Peritoneal macrophages were then
826 cultured in Atmospheric Media at pH 7.4 or 6.5 with 100µM D-luciferin, and kept at 37°C in atmospheric
827 conditions.
828
829 **Quantification of circadian rhythm parameters**
830 Using the Lumicycle Analysis program version 2.701 (Actimetrics), raw data was fitted to a linear
831 baseline, and the baseline-subtracted data was fitted to a damped sine wave from which period and
832 damping were calculated[140]. Amplitude was calculated from baseline-subtracted data by subtracting
833 the bioluminescent values of the first peak from the first trough as previously published[80].
834
835 **Production of KCKO cancer cell supernatant**
836 KCKO cells were seeded at 300,000 cells/mL in pH 7.4 Atmospheric Media (RPMI buffered for use at
837 atmospheric CO_2 levels and enhanced buffering capacity at low pH – see "Differentiation and culture of
838 bone marrow-derived macrophages" section) and cultured at 37°C in atmospheric conditions for 5 days.
839 Supernatant was then collected, pH-adjusted to pH 7.4 or pH 6.5, and filter-sterilized. For the
840 experiment, bone marrow-derived macrophages were cultured in pH 7.4 or pH 6.5 KCKO supernatant, or
841 pH 7.4 or pH 6.5 Atmospheric Media. Media was supplemented with 100 µM D-luciferin, and cells were
842 kept at 37°C in atmospheric conditions and monitored over time by LumiCycle
843
844 **Quantitative PCR**

845 Cells were lysed and RNA was isolated using the E.Z.N.A. HP Total RNA Kit (Omega BioTek, CAT#R6812-
846 02). RNA was reverse transcribed to cDNA using the ABI Reverse Transcription Reagents system, using
847 oligo dT for priming (Applied Biosystems, CAT#N8080234). qPCR was performed with cDNA using
848 PerfeCTa SYBR Green FastMix (QuantaBio, CAT#95074-05K) and with the Quant Studio 5 quantitative PCR
849 machines (Applied Biosystems). Triplicate technical replicates were performed, outlier replicates (defined
850 as being more than 1 Ct away from other two replicates) were discarded, and relative mRNA was
851 normalized to *Tbp* and assessed by the ΔΔCt. Primers used are in the **Table** below.

852 **Table of primer sequences used**

Target	Primer sequences (Forward, Reverse)	Source
Arg1	5'-CTCCAAGCCAAAGTCCTTAGAG-3', 5'-AGGAGCTGTCATTAGGGACATC-3'	[141]
Chil3	5'-AGAAGCAATCCTGAAGACACC-3', 5'-ACTGGTATAGTAGCACATCAGC-3'	IDT Mm.PT.58.33370435
Clec10a	5'-TGACTGAGTTCCTGCCTCT-3', 5'-GACCAAGGAGAGTGCTAGAAG-3'	IDT Mm.PT.56a.19092703
Cry1	5'-GCTATGCTCCTGGAGAGAACG T-3', 5'-TGTCCCCGTGAGCATAGTGTAA-3'	[142]
Icer	5'-ATGGCTGTAACTGGAGATGAA-3', 5'-GTGGCAAAGCAGTAGTAGGA-3'	[29]
Il1b	5'-TACGGACCCCAAAAGATGA-3', 5'-TGCTGCTGCGAGATTTGAAG-3'	[141]
Il6	5'-TAGTCCTTCCTACCCCAATTTCC-3', 5'-TTGGTCCTTAGCCACTCCTTC-3'	[141]

Mrc1	5'-CAAGTTGCCGTCTGAACTGA-3', 5'-TATCTCTGTCATCCCTGTCTCT-3'	IDT Mm.PT.58.42560062
Nos2	5'-GCTTCTGGTCGATGTCATGAG-3', 5'-TCCACCAGGAGATGTTGAAC-3'	IDT Mm.PT.58.43705194
Nr1d1	5'-GAGCCACTAGAGCCAATGTAG-3', 5'-CCAGTTTGAATGACCGCTTTC-3'	IDT Mm.PT.58.17472803
Per2	5'-TGAGGTAGATAGCCCAGGAG-3,' 5'-GCTATGAAGCGCCTAGAATCC-3'	IDT Mm.PT.58.5594166
Retnla	5'-CTGGGTTCTCCACCTCTTCA-3', 5'-TGCTGGGATGACTGCTACTG-3'	[141]
Tbp	5'-CCAGAACTGAAAATCAACGCAG-3', 5'-TGTATCTACCGTGAATCTTGGC-3'	IDT Mm.PT.39a.22214839
Tnfa	5'-ACGGCATGGATCTCAAAGAC-3', 5'-AGATAGCAAATCGGCTGACG-3'	[141]
Vegf	5'-CCACGACAGAAGGAGAGCAGAAGTCC-3', 5'-CGTTACAGCAGCCTGCACAGCG-3'	[93]

853

854 **Immunoblot**

855 Cells were lysed using the M-Per lysis reagent (Thermo Scientific, CAT#78501), supplemented with
856 protease and phosphatase inhibitor cocktail (1:100; Sigma, CAT#PPC1010) and phosphatase inhibitor
857 cocktail 2 (1:50; Sigma, CAT#P5726), with 200µM deferoxamine (Sigma, CAT#D9533). M-Per is
858 formulated to lyse the nucleus and solubilize nuclear and chromatin-bound proteins, allowing isolation
859 of nuclear proteins as well as cytosolic proteins. Lysates were incubated on ice for 1 hour, then
860 centrifuged at 17,000 xg to pellet out debris; supernatant was collected. Protein was quantified using the

861 Bio-Rad DC Protein Assay Kit (Bio-Rad, CAT#5000112), and lysates of equal concentration were prepared
862 and run by SDS-PAGE on Bio-Rad Criterion 4–15% Criterion TGX Stain-Free 26-well gradient gel (Bio-Rad,
863 CAT#5678095). Gels were transferred using the Trans-Blot Turbo system (Bio-Rad) to nitrocellulose
864 membranes (Bio-Rad CAT#1704271).
865
866 The following primary antibody was used: rabbit anti-p-CREB (Ser133, Ser129) (Invitrogen, CAT#44-
867 297G). The following secondary antibody was used: goat anti-rabbit Alexa Fluor 680 (Invitrogen,
868 CAT#A21109). Of note, two different anti-CREB antibodies were tested (Cell Signaling, CAT#9197 and
869 Invitrogen, CAT#35-0900) in combination with the appropriate secondary antibody, but neither revealed
870 bands at the correct molecular weight for CREB protein. Membranes were digitally imaged using a
871 ChemiDoc MP (Bio-Rad) and uniformly contrasted. Total protein was imaged by Stain-Free imaging
872 technology (Bio-Rad) and used as loading control. To visualize total protein, image of entire membrane
873 was shrunk to match the size of pCREB.
874
875 **Survival under acidic pH**
876 BMDMs were seeded, in triplicate, at $1.2*10^6$ cells/mL in a 96-well plate. BMDMs were synchronized,
877 then cultured in Atmospheric Media at pH 7.4, 6.8, or 6.5 containing 10 ng/mL IL-4 and 10 ng/mL IL-13,
878 or 50 ng/mL IFNγ and 100 ng/mL LPS, or vehicle for unstimulated control. BMDMs were fixed at 1, 2, and
879 3 days later. BMDMs were stained with Hoechst (Thermo Scientific, CAT#62259), and plates were imaged
880 using a Celigo S. Number of nuclei per well was enumerated using Celigo software to quantify the
881 number of adherent BMDMs after time in culture under acidic conditions as a readout of survival.
882
883 **Tumor growth**

884 Mice were anesthetized via inhalation of 4 vol% isoflurane (VetOne Fluriso) in 100% oxygen at a flow rate
885 of 4 L/min prior to injection. Following application of 70% ethanol to the site of injection, with $1*10^6$ WT
886 or BMAL1 KO macrophages and $1*10^6$ KCKO cells in 100 uL sterile 0.9% normal saline (Medline,
887 CAT#RDI30296) were subcutaneously co-injected in the flank of WT mice. In line with previously
888 published co-injection tumor experiments, mice were injected with macrophages at a 1:1 ratio[93, 109].
889 Tumor growth was measured by caliper, and volume was calculated by the modified ellipsoidal formula:
890 tumor volume = $0.5*(\text{length}*\text{width}^2)$[143]. Mice were euthanized when there was ulcer formation or
891 when tumor size reached a diameter of 20mm.
892
893 **Processing and analysis of publicly available bulk gene expression data**
894 FASTQ files from a previously published analysis of peritoneal macrophages cultured under neutral pH
895 7.4 or acidic pH 6.8 conditions were downloaded from NCBI GEO (accession #GSE164697)[30]. FASTQ
896 files from a previously published analysis of peritoneal macrophages from WT or BMAL1 KO mice were
897 downloaded from EMBL- European Bioinformatics Institute Array Express (accession #E-MTAB-8411)[44].
898 FASTQ files from a previously published analysis of bone marrow-derived macrophages were
899 downloaded from NCBI GEO (accession #GSE157878)[77]. FASTQ files from a previously published
900 analysis of macrophages from tumor and tumor-adjacent tissue from NSCLC patients were downloaded
901 from NCBI GEO (accession #GSE116946) [104]. FASTQ files from a previous published study of tumor-
902 associated macrophages were downloaded from NCBI GEO (accession #GSE188549)[101]. Where
903 applicable, multiple FASTQ files of the same run were concatenated before processing and mapping. CEL
904 files from a previously published microarray time series analysis of peritoneal macrophages from WT
905 mice were downloaded from NCBI GEO (accession #GSE25585)[36]. CEL files from a previously published
906 microarray analysis of alveolar macrophages from healthy human donors were downloaded from NCBI
907 GEO (accession #GSE13896)[105].

908

909 All FASTQ files were processed with FASTP using default parameters to trim adaptors and remove reads
910 that were low quality or too short[144]. Cleaned FASTQ files from mouse data were mapped to
911 transcripts using Salmon 1.3.0 in mapping-based mode using a decoy-aware transcription built from the
912 Gencode M27 GRCm39 primary assembly mouse genome and M27 mouse transcriptome, and from
913 human data were mapped to transcripts using Salmon 1.4.0 in mapping-based mode using a decoy-
914 aware transcription built from the Gencode v43 GRCh38 primary assembly human genome and v43
915 human transcriptome [145]. Single-end mapping was used for GSE188549, GSE116946 samples and
916 paired-end mapping was used for E-MTAB-8411 and GSE164697. All transcripts were then collapsed to
917 gene-level using Tximport v1.14.2 with the Gencode M27 transcriptome for mouse and the v43
918 transcriptome for human, and genes were annotated with symbols using the Ensembl GRCm39.104
919 transcriptome annotations for mouse and Ensembl GRCh38.111 transcriptome annotations for human
920 [146]. Transcripts per million (TPM) outputted from Tximport were used for downstream analyses.
921 Microarray data was imported and analyzed from CEL files using the packages affy and Limma, and genes
922 were annotated with symbols using the University of Michigan Brain Array Custom CDF v25.0 for the
923 Mouse Gene 1.0 ST Array or Human Gene 133 plus 2 Array[147, 148].

924

925 Clock correlation distance (CCD) analysis was performed as previously described[102]. Briefly, the default
926 universal 12-gene molecular circadian clock reference correlation was used. Genes outside this 12-gene
927 reference that were of zero variance across at least one of the sample groups were discarded prior to
928 analysis. For delta CCD, which directly compares between each group, the sample group with the lowest
929 CCD score (corresponding to the most ordered clock) was set as the control group, and $p<0.05$ was
930 deemed significantly different from the control group.

931

932 WCGNA analysis to determine significant co-variance between pairs of clock genes was performed as
933 previously described, using an expanded list of core circadian clock genes[101]. Results were calculated
934 from Pearson correlations of log-transformed TPM values. For data presented in Figure 6, the gene-
935 specific mean for TAMs within each group in the original publication (MHCII-high and MHCII-low, [101])
936 were subtracted out prior to analysis. Significance was determined by $p<0.05$ (Figure 6) or $p<0.01$ (Figure
937 7, Supplementary Figure 9).
938
939 **Processing and analysis of publicly available single-cell gene expression data**
940 A merged Seurat Object of single-cell RNA-sequencing data of immune cells infiltrating B16-F10
941 melanoma was downloaded from NCBI GEO (accession #GSE260641)[107]. Data were analyzed using
942 Seurat 5.0.3[149]. Macrophages, which were previously annotated, were isolated, gene expression
943 normalized, and the following factors regressed out: cell cycle state, mitochondrial content, and
944 circadian timepoint. 9 clusters were identified with the FindNeighbors and FindClusters commands.
945 UMAP was used to visualize macrophage clusters[150]. *Crem* high groups were identified from violin plot
946 and confirmed with differential expression compared to *Crem* low groups. All differential expression was
947 performed using the FindMarkers command only considering genes expressed within at least 10% of the
948 comparison populations and with a minimum log fold change of 0.25 between populations (min.pct = 0.1
949 and logfc.theshold = 0.25). Significantly differentially expressed genes were determined by adjusted
950 $p(adj.p)<0.05$ by the limma implementation of the Wilcoxon Rank Sum test (test.use =
951 "wilcox_limma")[147, 151]. A differentially expressed genes shown are $p(adj.p)<0.005$.
952
953 **Data sharing**
954 All raw data, analyses, and code used for analyses are available at FigShare at the following link:

955 https://rochester.figshare.com/projects/Source_data_for_Circadian_rhythms_of_macrophages_are_alte
956 red_by_the_acidic_pH_of_the_tumor_microenvironment/210625
957

958 ## Acknowledgements

959 We would like to thank Dr. Jim Miller (Department of Microbiology and Immunology, University of
960 Rochester) and Dr. Paul Brookes (Department of Anesthesiology and Perioperative Medicine, University
961 of Rochester) for their intellectual contributions. We also thank Dr. Christoph Scheiermann (University of
962 Geneva, Geneva, Switzerland) for assistance with scRNA-seq data, and the University of Rochester
963 Genomics Research Center (GRC) with assistance with data analysis and preparation. All visual
964 illustrations were made using BioRender. The project described was supported by Grant Number
965 T32AI007285 (to AMKC) from the National Institute of Allergy and Infectious Diseases of the National
966 Institutes of Health (NIH), Grant Number T32GM135134 (to AMKC) from the National Institute of
967 General Medical Sciences of the National Institutes of Health, Grant Numbers R00CA204593 and
968 R01CA282225 (to BJA) from the National Cancer Institute of the National Institutes of Health, the
969 University of Rochester University Research Award (to BJA), and the Wilmot Predoctoral Cancer Research
970 Fellowship (to AMKC) from the Wilmot Cancer Institute at the University of Rochester. The contents of
971 this paper are solely the responsibility of the Authors and do not necessarily represent the official views
972 of the NIH.
973

974 ## Author Contributions

975 Conceptualization: Amelia M. Knudsen-Clark, Brian J. Altman
976 Data Curation: Amelia M. Knudsen-Clark, Cameron Baker, Matthew M. McCall, Brian J. Altman
977 Formal analysis: Amelia M. Knudsen-Clark, Kristina Morris, Cameron Baker, Matthew M. McCall, Lauren
978 M. Hablitz, Brian J. Altman

979 Funding acquisition: Amelia M. Knudsen-Clark, Brian J. Altman

980 Investigation: Amelia M. Knudsen-Clark, Daniel Mwangi, Juliana Cazarin

981 Methodology: Amelia M. Knudsen-Clark, Kristina Morris, Minsoo Kim, Brian J. Altman

982 Resources: Brian J. Altman

983 Software: Amelia M. Knudsen-Clark, Daniel Mwangi, Kristina Morris, Cameron Baker, Matthew M.

984 McCall, Brian J. Altman

985 Supervision: Brian J. Altman

986 Validation: Amelia M. Knudsen-Clark

987 Visualization: Amelia M. Knudsen-Clark, Cameron Baker, Brian J. Altman

988 Writing – original draft: Amelia M. Knudsen-Clark

989 Writing – review and editing: Amelia M. Knudsen-Clark, Daniel Mwangi, Juliana Cazarin, Lauren M.

990 Hablitz, Minsoo Kim, Brian J. Altman

991

992 Conflict of Interest

993 The authors declare no conflict of interest.

994

995 Figure Legends

996 **Figure 1. Macrophages of different phenotypes have distinct circadian rhythms.** Bone marrow-derived

997 macrophages (BMDMs) were obtained from C57BL/6 mice expressing PER2-Luc. The circadian clocks of

998 BMDMs were synchronized by a 24-hour period of serum starvation in media with 0% serum, followed

999 by a 2-hour period of serum shock in media with 50% serum. Luciferase activity of BMDMs stimulated

1000 with either 10 ng/mL IL-4 and 10 ng/mL IL-13, or 50 ng/mL IFNγ and 100 ng/mL LPS; or left unstimulated

1001 was monitored in real time by LumiCycle. Data was baseline-subtracted using the running average.

1002 Oscillation parameters of BMDMs were measured by LumiCycle Analysis. Shown are mean and standard
1003 error of the mean (SEM), n=5 biological replicates. Statistical significance determined by unpaired two-
1004 tailed t-test with Welch's correction; *, $p < 0.05$; **, $p<0.005$; ***, $p<0.0005$. Data shown are
1005 representative of 2 independent experiments.
1006
1007 **Figure 2. Acidic pH alters circadian rhythms of bone marrow-derived macrophages *in vitro*. A-F**. Bone
1008 marrow-derived macrophages (BMDMs) were obtained from C57BL/6 mice expressing PER2-Luc. The
1009 circadian clocks of BMDMs were synchronized by a 24-hour period of serum starvation in media with 0%
1010 serum, followed by a 2-hour period of serum shock in media with 50% serum. BMDMs were then
1011 cultured in media with neutral pH 7.4 or acidic media with pH 6.8 or 6.5, and stimulated with either (**B,E**)
1012 10 ng/mL IL-4 and 10 ng/mL IL-13, or (**C,F**) 50 ng/mL IFNγ and 100 ng/mL LPS; or (**A,D**) left unstimulated.
1013 **A-C**. Luciferase activity was monitored in real time by LumiCycle. Shown are mean and SEM, n=2
1014 biological replicates, representative of 2 independent experiments. Data from both experiments was
1015 baseline-subtracted using the running average, and oscillation parameters were measured by LumiCycle
1016 Analysis. Shown are mean and SEM, n=5 biological replicates. **D-F**. In parallel, RNA was collected at 12,
1017 16, 20, and 24 hours post-synchronization, and qt-PCR was performed to assess oscillation of transcripts
1018 encoding core clock proteins in macrophages under acidic conditions. Shown are mean and SEM, n=3
1019 biological replicates. Data shown are representative of 2 independent experiments. Statistical
1020 significance determined by unpaired two-tailed t-test with Welch's correction; *, $p < 0.05$; **, $p<0.005$;
1021 ***, $p<0.0005$.
1022
1023 **Figure 3. Acidic pH alters circadian rhythms of peritoneal macrophages *ex vivo* at temporally distinct**
1024 **times of day. A,C**. Peritoneal macrophages were obtained at ZT0 or ZT12 from C57BL/6 mice expressing
1025 PER2-Luc and cultured in media with neutral pH 7.4 or acidic pH 6.5. **A**. Luciferase activity was monitored

1026 in real time by LumiCycle. Data was baseline-subtracted using the running average; shown is the mean
1027 and SEM, n=2, representative of 2 independent experiments. Oscillation parameters were measured by
1028 LumiCycle Analysis; shown is the mean and SEM, n=4, data pooled from 2 independent experiments. **B**.
1029 Clock gene expression, in transcripts per million (TPM), of peritoneal macrophages cultured in media at
1030 pH 7.4 or pH 6.8 for 24 hours, sourced from publicly available data (see **Methods**) shown is mean and
1031 SEM, n=3. **C**. The magnitude of change in circadian oscillation parameters between macrophages at pH
1032 7.4 and pH 6.5 was compared between peritoneal macrophages taken at ZT 0 or ZT 12. Shown is the
1033 mean and SEM, n=4; data pooled from 2 independent experiments. Statistical significance determined
1034 by paired two-tailed t-test with Welch's correction; *, $p < 0.05$; **, $p<0.005$; ***, $p<0.0005$.
1035
1036 **Figure 4. Lactate alters circadian rhythms in macrophages, both alone and in conjunction with acidic**
1037 **pH. A-C.** Bone marrow-derived macrophages (BMDMs) were obtained from C57BL/6 mice expressing
1038 PER2-Luc. The circadian clocks of BMDMs were synchronized by a 24-hour period of serum starvation in
1039 media with 0% serum, followed by a 2-hour period of serum shock in media with 50% serum. BMDMs
1040 were then cultured in media with neutral pH 7.4 or acidic pH 6.5, supplemented with 0 mM or 25 mM
1041 sodium-L-lactate. **A**. RNA was collected at 6 hours post-treatment, and expression of pro-resolution
1042 phenotype markers *Arg1* or *Vegf* was quantified by qt-PCR. Shown is the mean and SEM, n=6, data
1043 pooled from 2 independent experiments. **B**. Luciferase activity was monitored in real time by LumiCycle.
1044 Shown is the mean and SEM, n=4; data representative of 2 independent experiments. Data was baseline-
1045 subtracted using the running average, and oscillation parameters were measured by LumiCycle Analysis.
1046 Shown is the mean and SEM, n=7-10; data pooled from 2 independent experiments. **C**. RNA was
1047 collected at 12, 16, 20, and 24 hours post-synchronization, and qt-PCR was performed to assess
1048 oscillation of transcripts encoding core clock proteins in macrophages exposed to lactate. Shown is the
1049 mean and SEM, n=5-6; data pooled from 2 independent experiments. Statistical significance determined

1050 by unpaired two-tailed t-test with Welch's correction; *, $p < 0.05$; **, $p<0.005$; ***, $p<0.0005$; ****,
1051 $p<0.00005$.
1052
1053 **Figure 5. pH-induced changes in circadian rhythms are not driven by cAMP signaling alone. A-B**. Bone
1054 marrow-derived macrophages (BMDMs) were obtained from C57BL/6 mice expressing PER2-Luc.
1055 BMDMs were cultured in media with neutral pH 7.4 or acidic pH 6.5, and (**A**) treated with vehicle or 20,
1056 40 or 80 uM Forsokolin, or (**B**) treated with vehicle or 20, 40, 80 uM IBMX. Luciferase activity was
1057 monitored in real time by LumiCycle. Data was baseline-subtracted using the running average. Shown is
1058 the mean, n=2. **C.** The circadian clocks of BMDMs were synchronized by a 24-hour period of serum
1059 starvation in media with 0% serum, followed by a 2-hour period of serum shock in media with 50%
1060 serum. BMDMs were then cultured in media with neutral pH 7.4 or acidic pH 6.5, and treated with
1061 vehicle or 5, 10, or 15uM MDL-12330A (MDL-12). Luciferase activity was monitored in real time by
1062 LumiCycle. Data was baseline-subtracted using the running average, and oscillation parameters were
1063 measured by LumiCycle Analysis. Shown is the mean and SEM, n=4. **D.** Expression of genes associated
1064 with acid sensing (*Icer*) and pro-resolution phenotype (*Arg1*) was measured at 2 hours post-treatment
1065 (CT2). Shown is the mean and SEM; n=3. **E.** Phosphorylation of CREB was assessed by immunoblot at the
1066 indicated timepoints after synchronization, MDL-12 treatment, and exposure to low pH. **F.** Relative
1067 pCREB levels from (**E**) were quantified; band intensity was normalized to total protein, n=3. Statistical
1068 significance determined by unpaired two-tailed t-test with Welch's correction; *, $p < 0.05$; **, $p<0.005$;
1069 ***, $p<0.0005$; ****, $p<0.00005$. Data shown are representative of 2-3 independent experiments.
1070
1071 **Figure 6. Clock correlation distance (CCD) and weighted gene co-expression network analysis (WGCNA)**
1072 **provides evidence of circadian disorder in murine tumor-associated macrophages. A.** RNA-seq datasets
1073 (see **Methods**) of WT peritoneal macrophages, BMAL1 KO peritoneal macrophages, and tumor-

1074 associated macrophages (TAMs) were analyzed for expression of *Arg1* and *Crem*. **B.** A pan-tissue murine
1075 reference control was used for clock correlation distance (CCD). **C-D.** (**C**) Clock correlation distance (CCD)
1076 analysis was performed and (**D**) statistical analysis to compare CCD scores was performed by calculating
1077 delta CCD, with $p<0.05$ being deemed significantly different from the control group. **E**. Weighted gene
1078 co-expression network analysis (WGCNA) was performed on the indicated circadian clock genes using
1079 data from (**A-D**); asterisks represent significant covariance, where $p< 0.05$.
1080
1081 **Figure 7. Clock correlation distance (CCD) and weighted gene co-expression network analysis (WGCNA)**
1082 **provides evidence of circadian disorder in human tumor-associated macrophages. A.** Clock correlation
1083 distance (CCD) analysis was performed using RNA-seq datasets of macrophages from tumor (TAMs) and
1084 tumor-adjacent tissue from NSCLC patients and alveolar macrophages from healthy donors (see
1085 **Methods**). TAM samples were subset by median *Crem* expression into *Crem* high TAM samples (TAMs
1086 *Crem* high) and *Crem* low TAM samples (TAMs *Crem* low). **B.** Statistical analysis to compare CCD scores
1087 was performed by calculating delta CCD, with $p<0.05$ being deemed significantly different from the
1088 control group. **C.** Weighted gene co-expression network analysis (WGCNA) was performed on the
1089 indicated circadian clock genes using data from (**A-B**); asterisks represent significant covariance, where
1090 $p< 0.01$.
1091
1092 **Figure 8. Heterogeneity in circadian rhythms of cells within a population can lead to circadian disorder**
1093 **observed by CCD. A-C.** Increasingly desynchronized populations were modeled using an microarray data
1094 set of WT peritoneal macrophages (n=12) taken at 4-hour intervals across two days (see **Methods**). **A.** A
1095 schematic of the populations used in experimental design. **B-C.** (**B**) Clock correlation distance (CCD)
1096 analysis was performed and (**C**) statistical analysis to compare CCD scores was performed by calculating
1097 delta CCD, with $p<0.05$ being deemed significantly different from the control group.

1098

1099 **Figure 9. There is heterogeneity in expression of circadian clock genes within the tumor-associated**
1100 **macrophage population.** We analyzed a single-cell RNA-seq dataset of tumor-associated macrophages.
1101 **A.** Unbiased clustering was performed to identify TAM subpopulations. **B.** Differential gene expression
1102 analysis was performed on these TAM clusters, and expression of significantly different circadian genes
1103 was plotted along with *Crem*. **C.** Crem expression of macrophages in TAM clusters was measured. **D.**
1104 TAMs were subset by *Crem* expression into *Crem* high TAMs and *Crem* low TAMs, and these groups were
1105 overlaid on the UMAP plot shown in (**A**). **E.** Differential gene expression analysis was performed on *Crem*
1106 high vs *Crem* low, and expression of significantly different circadian genes was plotted. All differentially
1107 expressed genes or groups of clusters in (**B**), (**C**), and (**E**) are adj.p<0.005 by limma implementation of the
1108 Wilcoxon Rank Sum test.

1109

1110 **Figure 10. A functional circadian clock in macrophages can influence tumor growth in a murine model**
1111 **of PDAC.** Bone marrow-derived macrophages (BMDMs) obtained from WT or BMAL1 KO mice were
1112 subcutaneously co-injected with KCKO cells into the flank of WT mice. Tumor growth was measured by
1113 caliper. Shown is the mean and SEM; n=20 individual mice, 10 male and 10 female. Statistical significance
1114 determined at each time point by unpaired two-tailed t-test with Welch's correction; *, p < 0.05; **,
1115 p<0.005; ***, p<0.0005. Data shown are representative of 2 independent experiments.

1116

1117 **Supplementary Figure 1. Polarization of macrophages toward pro-resolution or pro-inflammatory**
1118 **phenotype.** Bone marrow-derived macrophages (BMDMs) were derived from C57BL/6 mice expressing
1119 PER2-Luc. The circadian clocks of BMDMs were synchronized by a 24-hour period of serum starvation in
1120 media with 0% serum, followed by a 2-hour period of serum shock in media with 50% serum. BMDMs
1121 were then stimulated with either 10 ng/mL IL-4 and 10 ng/mL IL-13, or 50 ng/mL IFNγ and 100 ng/mL

1122 LPS; or left unstimulated. RNA was collected at 6 hours post-synchronization, and qt-PCR was performed
1123 to assess expression of phenotype-associated genes. Shown are mean and standard error of the mean
1124 (SEM), n=3 biological replicates. Statistical significance determined by unpaired two-tailed t-test with
1125 Welch's correction; *, $p < 0.05$; **, ***, $p<0.0005$. Data shown are representative of 2 independent
1126 experiments.
1127
1128 **Supplementary Figure 2. The PER2-Luciferase reporter system enables real-time monitoring of**
1129 **circadian rhythms of macrophages. A.** A schematic of the PER2-Luciferase (PER2-Luc) luciferase reporter
1130 system. **B.** A schematic of the synchronization protocol in which the circadian clocks of bone marrow-
1131 derived macrophages (BMDMs) derived from C57BL/6 mice expressing PER2-Luc were synchronized by a
1132 24-hour period of serum starvation in media with 0% serum, followed by a 2-hour period of serum shock
1133 in media with 50% serum. **C.** BMDMs were then cultured in RPMI/10% FBS supplemented with D-
1134 luciferin at circadian time (CT) 0. Luciferase activity of BMDMs was monitored in real time by LumiCycle.
1135 **D-E.** Protein and RNA were collected at the indicated times post-serum shock to assess (**D**) cAMP
1136 signaling by p-CREB levels a€(**E**) expression of *Icer*. Statistical significance determined by unpaired two-
1137 tailed t-test with Welch's correction; **, $p < 0.005$. Data shown are representative of 2 independent
1138 experiments.
1139
1140 **Supplementary Figure 3. Macrophages sense and respond to an acidic extracellular environment when**
1141 **cultured *in vitro* in media with acidic pH. A-B.** Bone marrow-derived macrophages (BMDMs) were
1142 obtained from C57BL/6 mice expressing PER2-Luc. BMDMs were cultured in media with pH 7.4 or acidic
1143 media with pH 6.5, and stimulated with either 10 ng/mL IL-4 and 10 ng/mL IL-13, or 50 ng/mL IFNγ and
1144 100 ng/mL LPS; or left unstimulated. RNA was collected at 2 hours post-treatment, and qt-PCR was
1145 performed to assess expression of genes associated with (**A**) phenotype or (**B**) acid sensing in

1146 macrophages. Shown are mean and SEM, n=3 biological replicates. Statistical significance determined by
1147 two-tailed t-test with Welch's correction; *, $p < 0.05$; **, $p<0.005$; ***, $p<0.0005$; ****, $p<0.00005$. Data
1148 shown are representative of 2 independent experiments.
1149
1150 **Supplementary Figure 4. Survival of macrophages under acidic pH. A.** Lumicycle data from **Figure 2-A-C**
1151 are presented as axis-matched graphs. **B.** Bone marrow-derived macrophages (BMDMs) were obtained
1152 from C57BL/6 mice expressing PER2-Luc. The circadian clocks of BMDMs were synchronized by a 24-hour
1153 period of serum starvation in media with 0% serum, followed by a 2-hour period of serum shock in
1154 media with 50% serum. BMDMs were then cultured in media with pH 7.4 or acidic media with pH 6.8 or
1155 6.5, and stimulated with either 10 ng/mL IL-4 and 10 ng/mL IL-13, or 50 ng/mL IFNγ and 100 ng/mL LPS;
1156 or left unstimulated. Cells were fixed at CT 1, 2, and 3 days post-treatment and stained with DAPI.
1157 Number of nuclei was counted using Celigo to determine the number of adherent cells. **C.** Supernatant
1158 from (**A**) was collected at CT 12, 24, 36, and 48 hours and pH of media was measured. Shown is the
1159 mean and SEM, n=3. Statistical significance determined by multiple unpaired t-test with Welch's
1160 correction; *, $p < 0.05$; **, $p<0.005$; ***, $p<0.0005$. Data shown are representative of 2 independent
1161 experiments.
1162
1163 **Supplementary Figure 5. Exposure to cancer cell supernatant further modulates circadian rhythms in**
1164 **addition to pH-driven changes.** Bone marrow-derived macrophages (BMDMs) were obtained from
1165 C57BL/6 mice expressing PER2-Luc. The circadian clocks of BMDMs were synchronized by a 24-hour
1166 period of serum starvation in media with 0% serum, followed by a 2-hour period of serum shock in
1167 media with 50% serum. BMDMs were then cultured in RPMI with neutral pH 7.4 or acidic pH 6.5, or in
1168 KCKO supernatant at pH 6.5 or pH-adjusted to pH 7.4. Luciferase activity was monitored in real time by
1169 LumiCycle. Data was baseline-subtracted using the running average, and oscillation parameters were

1170 measured by LumiCycle Analysis. Shown is the mean and SEM, n=4. Statistical significance determined by
1171 unpaired two-tailed t-test with Welch's correction; *, $p < 0.05$; **, $p<0.005$; ***, $p<0.0005$; ****,
1172 $p<0.00005$.
1173
1174 **Supplementary Figure 6. Acidic pH alters circadian rhythms in macrophages in the absence of prior**
1175 **serum starvation followed by serum shock.** Bone marrow-derived macrophages (BMDMs) were
1176 obtained from C57BL/6 mice expressing PER2-Luc. BMDMs were cultured in media with neutral pH 7.4
1177 or acidic pH 6.8 or 6.5. Luciferase activity was monitored in real time by LumiCycle. Data was baseline-
1178 subtracted using the running average, and oscillation parameters were measured by LumiCycle Analysis.
1179 Shown is the mean and SEM, n=4-5. Data pooled from 2 individual experiments. Statistical significance
1180 determined by unpaired two-tailed t-test with Welch's correction; ***, $p<0.0005$; ****, $p<0.00005$.
1181
1182 **Supplementary Figure 7. Pre-treatment with 15 uM MDL-12 for up to 2 hours is not necessary to**
1183 **suppress pH-driven changes in amplitude of circadian rhythms. A-E.** Bone marrow-derived
1184 macrophages (BMDMs) were obtained from C57BL/6 mice expressing PER2-Luc. The circadian clocks of
1185 BMDMs were synchronized by a 24-hour period of serum starvation in media with 0% serum, followed
1186 by a 2-hour period of serum shock in media with 50% serum. (**A**) BMDMs were then cultured in media
1187 with neutral pH 7.4 or acidic pH 6.5, and treated with vehicle or 15uM MDL-12. Alternately, (**B,C**)
1188 BMDMs were cultured at pH 7.4 and pre-treated with 15uM MDL-12 for 30 minutes or (**D,E**) 2 hours,
1189 after which media was removed and cells were cultured in media at pH 7.4 or pH 6.5 in the (**C,E**)
1190 presence or (**B,D**) absence of MDL-12. Luciferase activity was monitored in real time by LumiCycle.
1191 Shown is the mean, n=2 biological replicates. Data for cells that received no pre-treatment (**A**) was
1192 overlaid on plots of data where cells received pre-treatment (**B-E**) to allow for comparison of changes in
1193 rhythms.

1194

1195 **Supplementary Figure 8. Macrophages from BMAL1 KO mice have disrupted circadian rhythms. A.**

1196 Levels of Bmal1 in bone marrow-derived macrophages (BMDMs) from WT or BMAL1 KO mice were

1197 assessed by immunoblot. **B.** To confirm functional disruption of the circadian clock, peritoneal

1198 macrophages or BMDMs were obtained from WT or BMAL1 KO mice expressing PER2-Luc and cultured *in*

1199 *vitro* with D-luciferin. Luciferase activity was monitored in real time by LumiCycle. Shown is the mean

1200 and SEM, n=2, representative of 2 independent experiments.

1201

1202 **Supplementary Figure 9. Heterogeneity in circadian rhythms of cells within a population can lead to an**

1203 **altered circadian clock gene network in samples.** Increasingly desynchronized populations were

1204 modeled using an RNA-seq data set of WT peritoneal macrophages taken at 4-hour intervals across two

1205 days (see **Methods**). Weighted gene co-expression network analysis (WGCNA) was performed; asterisks

1206 represent significant covariance, where $p < 0.01$.

1207

1208 # References

1209

1210 1. Cassetta, L. and J.W. Pollard, *Targeting macrophages: therapeutic approaches in cancer.* Nat Rev
1211 Drug Discov, 2018. **17**(12): p. 887-904.
1212 2. Zhang, Q.W., et al., *Prognostic significance of tumor-associated macrophages in solid tumor: a*
1213 *meta-analysis of the literature.* PLoS One, 2012. **7**(12): p. e50946.
1214 3. Gentles, A.J., et al., *The prognostic landscape of genes and infiltrating immune cells across*
1215 *human cancers.* Nat Med, 2015. **21**(8): p. 938-945.
1216 4. DeNardo, D.G. and B. Ruffell, *Macrophages as regulators of tumour immunity and*
1217 *immunotherapy.* Nat Rev Immunol, 2019.
1218 5. Mosser, D.M. and J.P. Edwards, *Exploring the full spectrum of macrophage activation.* Nat Rev
1219 Immunol, 2008. **8**(12): p. 958-69.
1220 6. Murray, P.J. and T.A. Wynn, *Protective and pathogenic functions of macrophage subsets.* Nat Rev
1221 Immunol, 2011. **11**(11): p. 723-37.
1222 7. Coussens, L.M. and Z. Werb, *Inflammation and cancer.* Nature, 2002. **420**(6917): p. 860-7.
1223 8. Murray, P.J., *Nonresolving macrophage-mediated inflammation in malignancy.* Febs j, 2018.
1224 **285**(4): p. 641-653.
1225 9. Schoppmann, S.F., et al., *Tumor-associated macrophages express lymphatic endothelial growth*
1226 *factors and are related to peritumoral lymphangiogenesis.* Am J Pathol, 2002. **161**(3): p. 947-56.
1227 10. Huber, R., et al., *Tumour hypoxia promotes melanoma growth and metastasis via High Mobility*
1228 *Group Box-1 and M2-like macrophages.* Sci Rep, 2016. **6**: p. 29914.
1229 11. Graham, D.K., et al., *The TAM family: phosphatidylserine sensing receptor tyrosine kinases gone*
1230 *awry in cancer.* Nat Rev Cancer, 2014. **14**(12): p. 769-85.
1231 12. Cook, R.S., et al., *MerTK inhibition in tumor leukocytes decreases tumor growth and metastasis.* J
1232 Clin Invest, 2013. **123**(8): p. 3231-42.
1233 13. Roberts, A.W., et al., *Tissue-Resident Macrophages Are Locally Programmed for Silent Clearance*
1234 *of Apoptotic Cells.* Immunity, 2017. **47**(5): p. 913-927.e6.
1235 14. Fadok, V.A., et al., *Macrophages that have ingested apoptotic cells in vitro inhibit*
1236 *proinflammatory cytokine production through autocrine/paracrine mechanisms involving TGF-*
1237 *beta, PGE2, and PAF.* J Clin Invest, 1998. **101**(4): p. 890-8.
1238 15. Strassmann, G., et al., *Evidence for the involvement of interleukin 10 in the differential*
1239 *deactivation of murine peritoneal macrophages by prostaglandin E2.* J Exp Med, 1994. **180**(6): p.
1240 2365-70.
1241 16. Kuang, D.M., et al., *Activated monocytes in peritumoral stroma of hepatocellular carcinoma*
1242 *foster immune privilege and disease progression through PD-L1.* J Exp Med, 2009. **206**(6): p.
1243 1327-37.
1244 17. Ruffell, B. and L.M. Coussens, *Macrophages and therapeutic resistance in cancer.* Cancer Cell,
1245 2015. **27**(4): p. 462-72.
1246 18. Mantovani, A., et al., *Macrophages as tools and targets in cancer therapy.* Nature Reviews Drug
1247 Discovery, 2022. **21**(11): p. 799-820.
1248 19. Cuccarese, M.F., et al., *Heterogeneity of macrophage infiltration and therapeutic response in*
1249 *lung carcinoma revealed by 3D organ imaging.* Nat Commun, 2017. **8**: p. 14293.
1250 20. Chevrier, S., et al., *An Immune Atlas of Clear Cell Renal Cell Carcinoma.* Cell, 2017. **169**(4): p. 736-
1251 749.e18.

1252 21. Laviron, M., et al., *Tumor-associated macrophage heterogeneity is driven by tissue territories in*
1253 *breast cancer.* Cell Rep, 2022. **39**(8): p. 110865.
1254 22. Nalio Ramos, R., et al., *Tissue-resident FOLR2(+) macrophages associate with CD8(+) T cell*
1255 *infiltration in human breast cancer.* Cell, 2022. **185**(7): p. 1189-1207.e25.
1256 23. Yano, S., et al., *Spatial-temporal FUCCI imaging of each cell in a tumor demonstrates locational*
1257 *dependence of cell cycle dynamics and chemoresponsiveness.* Cell Cycle, 2014. **13**(13): p. 2110-9.
1258 24. Huang, Y.K., et al., *Macrophage spatial heterogeneity in gastric cancer defined by multiplex*
1259 *immunohistochemistry.* Nat Commun, 2019. **10**(1): p. 3928.
1260 25. Lyssiotis, C.A. and A.C. Kimmelman, *Metabolic Interactions in the Tumor Microenvironment.*
1261 Trends Cell Biol, 2017. **27**(11): p. 863-875.
1262 26. Raghunand, N., R.A. Gatenby, and R.J. Gillies, *Microenvironmental and cellular consequences of*
1263 *altered blood flow in tumours.* Br J Radiol, 2003. **76 Spec No 1**: p. S11-22.
1264 27. Gillies, R.J., et al., *Targeting acidity in cancer and diabetes.* Biochim Biophys Acta Rev Cancer,
1265 2019. **1871**(2): p. 273-280.
1266 28. El-Kenawi, A., et al., *Acidity promotes tumour progression by altering macrophage phenotype in*
1267 *prostate cancer.* Br J Cancer, 2019. **121**(7): p. 556-566.
1268 29. Bohn, T., et al., *Tumor immunoevasion via acidosis-dependent induction of regulatory tumor-*
1269 *associated macrophages.* Nat Immunol, 2018. **19**(12): p. 1319-1329.
1270 30. Jiang, W., et al., *Extracellular Acidity Reprograms Macrophage Metabolism and Innate*
1271 *Responsiveness.* The Journal of Immunology, 2021. **206**(12): p. 3021-3031.
1272 31. Partch, C.L., C.B. Green, and J.S. Takahashi, *Molecular architecture of the mammalian circadian*
1273 *clock.* Trends Cell Biol, 2014. **24**(2): p. 90-9.
1274 32. Walton, Z.E., et al., *Acid Suspends the Circadian Clock in Hypoxia through Inhibition of mTOR.*
1275 Cell, 2018. **174**(1): p. 72-87.e32.
1276 33. Mure, L.S., et al., *Diurnal transcriptome atlas of a primate across major neural and peripheral*
1277 *tissues.* Science, 2018. **359**(6381).
1278 34. Zhang, R., et al., *A circadian gene expression atlas in mammals: implications for biology and*
1279 *medicine.* Proc Natl Acad Sci U S A, 2014. **111**(45): p. 16219-24.
1280 35. Haspel, J.A., et al., *Perfect timing: circadian rhythms, sleep, and immunity - an NIH workshop*
1281 *summary.* JCI Insight, 2020. **5**(1).
1282 36. Keller, M., et al., *A circadian clock in macrophages controls inflammatory immune responses.*
1283 Proc Natl Acad Sci U S A, 2009. **106**(50): p. 21407-12.
1284 37. Silver, A.C., et al., *Circadian expression of clock genes in mouse macrophages, dendritic cells, and*
1285 *B cells.* Brain Behav Immun, 2012. **26**(3): p. 407-13.
1286 38. Nguyen, K.D., et al., *Circadian gene Bmal1 regulates diurnal oscillations of Ly6C(hi) inflammatory*
1287 *monocytes.* Science, 2013. **341**(6153): p. 1483-8.
1288 39. Baumann, A., et al., *The circadian clock is functional in eosinophils and mast cells.* Immunology,
1289 2013. **140**(4): p. 465-74.
1290 40. Adrover, J.M., et al., *A Neutrophil Timer Coordinates Immune Defense and Vascular Protection.*
1291 Immunity, 2019. **50**(2): p. 390-402.e10.
1292 41. Arjona, A. and D.K. Sarkar, *Circadian oscillations of clock genes, cytolytic factors, and cytokines in*
1293 *rat NK cells.* J Immunol, 2005. **174**(12): p. 7618-24.
1294 42. Druzd, D., et al., *Lymphocyte Circadian Clocks Control Lymph Node Trafficking and Adaptive*
1295 *Immune Responses.* Immunity, 2017. **46**(1): p. 120-132.
1296 43. Scheiermann, C., et al., *Clocking in to immunity.* Nat Rev Immunol, 2018. **18**(7): p. 423-437.
1297 44. Kitchen, G.B., et al., *The clock gene Bmal1 inhibits macrophage motility, phagocytosis, and*
1298 *impairs defense against pneumonia.* Proc Natl Acad Sci U S A, 2020.

45. Gibbs, J.E., et al., *The nuclear receptor REV-ERBalpha mediates circadian regulation of innate immunity through selective regulation of inflammatory cytokines.* Proc Natl Acad Sci U S A, 2012. **109**(2): p. 582-7.
46. He, W., et al., *Circadian Expression of Migratory Factors Establishes Lineage-Specific Signatures that Guide the Homing of Leukocyte Subsets to Tissues.* Immunity, 2018. **49**(6): p. 1175-1190.e7.
47. Nobis, C.C., et al., *The circadian clock of CD8 T cells modulates their early response to vaccination and the rhythmicity of related signaling pathways.* Proc Natl Acad Sci U S A, 2019. **116**(40): p. 20077-20086.
48. Fortier, E.E., et al., *Circadian variation of the response of T cells to antigen.* J Immunol, 2011. **187**(12): p. 6291-300.
49. Beam, C.A., et al., *Synchronization of the Normal Human Peripheral Immune System: A Comprehensive Circadian Systems Immunology Analysis.* Sci Rep, 2020. **10**(1): p. 672.
50. Mazzoccoli, G., et al., *A timetable of 24-hour patterns for human lymphocyte subpopulations.* J Biol Regul Homeost Agents, 2011. **25**(3): p. 387-95.
51. Silver, A.C., et al., *The circadian clock controls toll-like receptor 9-mediated innate and adaptive immunity.* Immunity, 2012. **36**(2): p. 251-61.
52. Phillips, A.C., et al., *Preliminary evidence that morning vaccination is associated with an enhanced antibody response in men.* Psychophysiology, 2008. **45**(4): p. 663-6.
53. Long, J.E., et al., *Morning vaccination enhances antibody response over afternoon vaccination: A cluster-randomised trial.* Vaccine, 2016. **34**(24): p. 2679-85.
54. Curtis, A.M., et al., *Circadian control of innate immunity in macrophages by miR-155 targeting Bmal1.* Proc Natl Acad Sci U S A, 2015. **112**(23): p. 7231-6.
55. Deng, W., et al., *The Circadian Clock Controls Immune Checkpoint Pathway in Sepsis.* Cell Rep, 2018. **24**(2): p. 366-378.
56. Aiello, I., et al., *Circadian disruption promotes tumor-immune microenvironment remodeling favoring tumor cell proliferation.* Sci Adv, 2020. **6**(42).
57. Tsuruta, A., et al., *Diurnal Expression of PD-1 on Tumor-Associated Macrophages Underlies the Dosing Time-Dependent Antitumor Effects of the PD-1/PD-L1 Inhibitor BMS-1 in B16/BL6 Melanoma-Bearing Mice.* Mol Cancer Res, 2022. **20**(6): p. 972-982.
58. Strauss, L., et al., *Targeted deletion of PD-1 in myeloid cells induces antitumor immunity.* Sci Immunol, 2020. **5**(43).
59. Qian, D.C., et al., *Effect of immunotherapy time-of-day infusion on overall survival among patients with advanced melanoma in the USA (MEMOIR): a propensity score-matched analysis of a single-centre, longitudinal study.* Lancet Oncol, 2021. **22**(12): p. 1777-1786.
60. Munder, M., K. Eichmann, and M. Modolell, *Alternative metabolic states in murine macrophages reflected by the nitric oxide synthase/arginase balance: competitive regulation by CD4+ T cells correlates with Th1/Th2 phenotype.* J Immunol, 1998. **160**(11): p. 5347-54.
61. Murray, P.J., *Macrophage Polarization.* Annual Review of Physiology, 2017. **79**(Volume 79, 2017): p. 541-566.
62. Biswas, S.K. and A. Mantovani, *Macrophage plasticity and interaction with lymphocyte subsets: cancer as a paradigm.* Nat Immunol, 2010. **11**(10): p. 889-96.
63. Viola, A., et al., *The Metabolic Signature of Macrophage Responses.* Front Immunol, 2019. **10**: p. 1462.
64. Nathan, C.F., et al., *Identification of interferon-gamma as the lymphokine that activates human macrophage oxidative metabolism and antimicrobial activity.* J Exp Med, 1983. **158**(3): p. 670-89.
65. Hörhold, F., et al., *Reprogramming of macrophages employing gene regulatory and metabolic network models.* PLOS Computational Biology, 2020. **16**(2): p. e1007657.

66. Mills, C.D., et al., *M-1/M-2 macrophages and the Th1/Th2 paradigm.* J Immunol, 2000. **164**(12): p. 6166-73.
67. Stein, M., et al., *Interleukin 4 potently enhances murine macrophage mannose receptor activity: a marker of alternative immunologic macrophage activation.* J Exp Med, 1992. **176**(1): p. 287-92.
68. Allen, J.E., *IL-4 and IL-13: Regulators and Effectors of Wound Repair.* Annu Rev Immunol, 2023. **41**: p. 229-254.
69. Mantovani, A., et al., *Macrophage plasticity and polarization in tissue repair and remodelling.* J Pathol, 2013. **229**(2): p. 176-85.
70. Pesce, J.T., et al., *Retnla (relmalpha/fizz1) suppresses helminth-induced Th2-type immunity.* PLoS Pathog, 2009. **5**(4): p. e1000393.
71. McWhorter, F.Y., et al., *Modulation of macrophage phenotype by cell shape.* Proc Natl Acad Sci U S A, 2013. **110**(43): p. 17253-8.
72. Biswas, S.K., et al., *A distinct and unique transcriptional program expressed by tumor-associated macrophages (defective NF-kappaB and enhanced IRF-3/STAT1 activation).* Blood, 2006. **107**(5): p. 2112-22.
73. Ding, C., et al., *Tumor Microenvironment Modulates Immunological Outcomes of Myeloid Cells with mTORC1 Disruption.* J Immunol, 2019. **202**(5): p. 1623-1634.
74. Martinez, F.O. and S. Gordon, *The M1 and M2 paradigm of macrophage activation: time for reassessment.* F1000Prime Rep, 2014. **6**: p. 13.
75. Binger, K.J., et al., *High salt reduces the activation of IL-4– and IL-13–stimulated macrophages.* The Journal of Clinical Investigation, 2015. **125**(11): p. 4223-4238.
76. Yoo, S.H., et al., *PERIOD2::LUCIFERASE real-time reporting of circadian dynamics reveals persistent circadian oscillations in mouse peripheral tissues.* Proc Natl Acad Sci U S A, 2004. **101**(15): p. 5339-46.
77. Collins, E.J., et al., *Post-transcriptional circadian regulation in macrophages organizes temporally distinct immunometabolic states.* Genome Res, 2021. **31**(2): p. 171-85.
78. Rodheim, K., C. Jung, and K. Wright, *016 Associations between Circadian Melatonin and Temperature Amplitudes during Constant Routine.* Sleep, 2021. **44**(Supplement_2): p. A8-A8.
79. Wu, G., et al., *Normalized coefficient of variation (nCV): a method to evaluate circadian clock robustness in population scale data.* Bioinformatics, 2021. **37**(23): p. 4581-4583.
80. Chen, S., et al., *A Pro- and Anti-inflammatory Axis Modulates the Macrophage Circadian Clock.* Front Immunol, 2020. **11**: p. 867.
81. Lellupitiyage Don, S.S., et al., *Macrophage circadian rhythms are differentially affected based on stimuli.* Integr Biol (Camb), 2022. **14**(3): p. 62-75.
82. Pilorz, V., et al., *A Novel Mechanism Controlling Resetting Speed of the Circadian Clock to Environmental Stimuli.* Current Biology, 2014. **24**(7): p. 766-773.
83. Abe, M., et al., *Circadian rhythms in isolated brain regions.* J Neurosci, 2002. **22**(1): p. 350-6.
84. Gaspar, L.S., et al., *The importance of determining circadian parameters in pharmacological studies.* British Journal of Pharmacology, 2019. **176**(16): p. 2827-2847.
85. Boedtkjer, E. and S.F. Pedersen, *The Acidic Tumor Microenvironment as a Driver of Cancer.* Annual Review of Physiology, 2020. **82**(1): p. 103-126.
86. Gillies, R.J., Z. Liu, and Z. Bhujwalla, *31P-MRS measurements of extracellular pH of tumors using 3-aminopropylphosphonate.* Am J Physiol, 1994. **267**(1 Pt 1): p. C195-203.
87. Estrella, V., et al., *Acidity Generated by the Tumor Microenvironment Drives Local Invasion.* Cancer Research, 2013. **73**(5): p. 1524-1535.
88. Lv, S., et al., *A negative feedback loop of ICER and NF-κB regulates TLR signaling in innate immune responses.* Cell Death Differ, 2017. **24**(3): p. 492-499.
89. Kraut, J.A. and N.E. Madias, *Lactic acidosis.* N Engl J Med, 2014. **371**(24): p. 2309-19.

1394 90. Pastorekova, S. and R.J. Gillies, *The role of carbonic anhydrase IX in cancer development: links to*
1395 *hypoxia, acidosis, and beyond.* Cancer Metastasis Rev, 2019. **38**(1-2): p. 65-77.
1396 91. Swietach, P., *What is pH regulation, and why do cancer cells need it?* Cancer Metastasis Rev,
1397 2019. **38**(1-2): p. 5-15.
1398 92. de la Cruz-López, K.G., et al., *Lactate in the Regulation of Tumor Microenvironment and*
1399 *Therapeutic Approaches.* Front Oncol, 2019. **9**: p. 1143.
1400 93. Colegio, O.R., et al., *Functional polarization of tumour-associated macrophages by tumour-*
1401 *derived lactic acid.* Nature, 2014. **513**(7519): p. 559-63.
1402 94. Kidiyoor, A., et al., *Pancreatic Cancer Cells Isolated from Muc1-Null Tumors Favor the Generation*
1403 *of a Mature Less Suppressive MDSC Population.* Front Immunol, 2014. **5**: p. 67.
1404 95. Besmer, D.M., et al., *Pancreatic ductal adenocarcinoma mice lacking mucin 1 have a profound*
1405 *defect in tumor growth and metastasis.* Cancer Res, 2011. **71**(13): p. 4432-42.
1406 96. Polumuri, S., D.J. Perkins, and S.N. Vogel, *cAMP levels regulate macrophage alternative*
1407 *activation marker expression.* Innate Immun, 2021. **27**(2): p. 133-142.
1408 97. Tavares, L.P., et al., *Blame the signaling: Role of cAMP for the resolution of inflammation.*
1409 Pharmacol Res, 2020. **159**: p. 105030.
1410 98. Yagita, K. and H. Okamura, *Forskolin induces circadian gene expression of rPer1, rPer2 and dbp in*
1411 *mammalian rat-1 fibroblasts.* FEBS Lett, 2000. **465**(1): p. 79-82.
1412 99. O'Neill, J.S., et al., *cAMP-dependent signaling as a core component of the mammalian circadian*
1413 *pacemaker.* Science, 2008. **320**(5878): p. 949-53.
1414 100. Misra, U.K. and S.V. Pizzo, *Coordinate regulation of forskolin-induced cellular proliferation in*
1415 *macrophages by protein kinase A/cAMP-response element-binding protein (CREB) and Epac1-*
1416 *Rap1 signaling: effects of silencing CREB gene expression on Akt activation.* J Biol Chem, 2005.
1417 **280**(46): p. 38276-89.
1418 101. Geeraerts, X., et al., *Macrophages are metabolically heterogeneous within the tumor*
1419 *microenvironment.* Cell Rep, 2021. **37**(13): p. 110171.
1420 102. Shilts, J., G. Chen, and J.J. Hughey, *Evidence for widespread dysregulation of circadian clock*
1421 *progression in human cancer.* PeerJ, 2018. **6**: p. e4327.
1422 103. Chun, S.K., et al., *Disruption of the circadian clock drives Apc loss of heterozygosity to accelerate*
1423 *colorectal cancer.* Sci Adv, 2022. **8**(32): p. eabo2389.
1424 104. Garrido-Martin, E.M., et al., *M1(hot) tumor-associated macrophages boost tissue-resident*
1425 *memory T cells infiltration and survival in human lung cancer.* J Immunother Cancer, 2020. **8**(2).
1426 105. Shaykhiev, R., et al., *Smoking-dependent reprogramming of alveolar macrophage polarization:*
1427 *implication for pathogenesis of chronic obstructive pulmonary disease.* J Immunol, 2009. **183**(4):
1428 p. 2867-83.
1429 106. Pariollaud, M., et al., *Circadian disruption enhances HSF1 signaling and tumorigenesis in Kras-*
1430 *driven lung cancer.* Science Advances, 2022. **8**(39): p. eabo1123.
1431 107. Wang, C., et al., *Circadian tumor infiltration and function of CD8+ T cells dictate immunotherapy*
1432 *efficacy.* Cell, 2024. **187**(11): p. 2690-2702.e17.
1433 108. Mills, B.N., et al., *Stereotactic Body Radiation and Interleukin-12 Combination Therapy Eradicates*
1434 *Pancreatic Tumors by Repolarizing the Immune Microenvironment.* Cell Rep, 2019. **29**(2): p. 406-
1435 421.e5.
1436 109. Alexander, R.K., et al., *Bmal1 integrates mitochondrial metabolism and macrophage activation.*
1437 eLife, 2020. **9**: p. e54090.
1438 110. Lee, C.-C., et al., *Macrophage-secreted interleukin-35 regulates cancer cell plasticity to facilitate*
1439 *metastatic colonization.* Nature Communications, 2018. **9**(1): p. 3763.
1440 111. Certo, M., et al., *Understanding lactate sensing and signalling.* Trends Endocrinol Metab, 2022.
1441 **33**(10): p. 722-735.

1442 112. Liu, C., et al., *Transcriptional coactivator PGC-1alpha integrates the mammalian clock and energy*
1443 *metabolism.* Nature, 2007. **447**(7143): p. 477-81.
1444 113. Odegaard, J.I., et al., *Macrophage-specific PPARγ controls alternative activation and improves*
1445 *insulin resistance.* Nature, 2007. **447**(7148): p. 1116-1120.
1446 114. Daniel, B., et al., *The Nuclear Receptor PPARγ Controls Progressive Macrophage Polarization as a*
1447 *Ligand-Insensitive Epigenomic Ratchet of Transcriptional Memory.* Immunity, 2018. **49**(4): p. 615-
1448 626.e6.
1449 115. Gautier, E.L., et al., *Systemic analysis of PPARγ in mouse macrophage populations reveals marked*
1450 *diversity in expression with critical roles in resolution of inflammation and airway immunity.* J
1451 Immunol, 2012. **189**(5): p. 2614-24.
1452 116. Walton, Z.E., R.C. Brooks, and C.V. Dang, *mTOR Senses Intracellular pH through Lysosome*
1453 *Dispersion from RHEB.* Bioessays, 2019: p. e1800265.
1454 117. Guellaen, G., et al., *RMI 12330 A, an inhibitor of adenylate cyclase in rat liver.* Biochim Biophys
1455 Acta, 1977. **484**(2): p. 465-75.
1456 118. Hunt, N.H. and T. Evans, *RMI 12330A, an inhibitor of cyclic nucleotide phosphodiesterases and*
1457 *adenylate cyclase in kidney preparations.* Biochim Biophys Acta, 1980. **613**(2): p. 499-506.
1458 119. van Rossum, D.B., et al., *Ca2+ entry mediated by store depletion, S-nitrosylation, and TRP3*
1459 *channels. Comparison of coupling and function.* J Biol Chem, 2000. **275**(37): p. 28562-8.
1460 120. O'Neill, J.S. and A.B. Reddy, *The essential role of cAMP/Ca2+ signalling in mammalian circadian*
1461 *timekeeping.* Biochem Soc Trans, 2012. **40**(1): p. 44-50.
1462 121. Ni, L., et al., *Identification and Function of Acid-sensing Ion Channels in RAW 264.7 Macrophage*
1463 *Cells.* Curr Med Sci, 2018. **38**(3): p. 436-442.
1464 122. Selezneva, A., A.J. Gibb, and D. Willis, *The contribution of ion channels to shaping macrophage*
1465 *behaviour.* Front Pharmacol, 2022. **13**: p. 970234.
1466 123. Finger, A.M., et al., *Intercellular coupling between peripheral circadian oscillators by TGF-β*
1467 *signaling.* Sci Adv, 2021. **7**(30).
1468 124. Massagué, J., *TGFb in Cancer.* Cell, 2008. **134**(2): p. 215-230.
1469 125. Lavin, Y., et al., *Innate Immune Landscape in Early Lung Adenocarcinoma by Paired Single-Cell*
1470 *Analyses.* Cell, 2017. **169**(4): p. 750-765.e17.
1471 126. Storrs, E.P., et al., *High-dimensional deconstruction of pancreatic cancer identifies tumor*
1472 *microenvironmental and developmental stemness features that predict survival.* NPJ Precis
1473 Oncol, 2023. **7**(1): p. 105.
1474 127. Takahashi, J.S., *Transcriptional architecture of the mammalian circadian clock.* Nat Rev Genet,
1475 2017. **18**(3): p. 164-179.
1476 128. Kato, Y., et al., *Chapter Ten - DEC1/STRA13/SHARP2 and DEC2/SHARP1 Coordinate Physiological*
1477 *Processes, Including Circadian Rhythms in Response to Environmental Stimuli*, in *Current Topics in*
1478 *Developmental Biology*, R. Taneja, Editor. 2014, Academic Press. p. 339-372.
1479 129. Sato, S., et al., *A circadian clock gene, Rev-erbalpha, modulates the inflammatory function of*
1480 *macrophages through the negative regulation of Ccl2 expression.* J Immunol, 2014. **192**(1): p.
1481 407-17.
1482 130. Billon, C., et al., *RORγ regulates the NLRP3 inflammasome.* Journal of Biological Chemistry, 2019.
1483 **294**(1): p. 10-19.
1484 131. Geiger, S.S., et al., *Daily variation in macrophage phagocytosis is clock-independent and*
1485 *dispensable for cytokine production.* Immunology, 2019.
1486 132. Committee, N.R.C., *Guide for the Care and Use of Laboratory Animals*, in *Guide for the Care and*
1487 *Use of Laboratory Animals*. 2011, National Academies Press (US)
1488 Copyright © 2011, National Academy of Sciences.: Washington (DC).

133. Clausen, B.E., et al., *Conditional gene targeting in macrophages and granulocytes using LysMcre mice.* Transgenic Res, 1999. **8**(4): p. 265-77.
134. Storch, K.F., et al., *Intrinsic circadian clock of the mammalian retina: importance for retinal processing of visual information.* Cell, 2007. **130**(4): p. 730-741.
135. Trouplin, V., et al., *Bone marrow-derived macrophage production.* J Vis Exp, 2013(81): p. e50966.
136. Gonçalves, R. and D.M. Mosser, *The Isolation and Characterization of Murine Macrophages.* Current Protocols in Immunology, 2015. **111**(1): p. 14.1.1-14.1.16.
137. Ray, A. and B.N. Dittel, *Isolation of mouse peritoneal cavity cells.* J Vis Exp, 2010(35).
138. Layoun, A., M. Samba, and M.M. Santos, *Isolation of murine peritoneal macrophages to carry out gene expression analysis upon Toll-like receptors stimulation.* J Vis Exp, 2015(98): p. e52749.
139. De Jesus, A., et al., *Optimized protocol to isolate primary mouse peritoneal macrophage metabolites.* STAR Protoc, 2022. **3**(4): p. 101668.
140. Ramanathan, C., et al., *Cell Type-Specific Functions of Period Genes Revealed by Novel Adipocyte and Hepatocyte Circadian Clock Models.* PLOS Genetics, 2014. **10**(4): p. e1004244.
141. Liu, P.S., et al., *alpha-ketoglutarate orchestrates macrophage activation through metabolic and epigenetic reprogramming.* Nat Immunol, 2017. **18**(9): p. 985-994.
142. Huber, A.L., et al., *CRY2 and FBXL3 Cooperatively Degrade c-MYC.* Mol Cell, 2016. **64**(4): p. 774-789.
143. Tomayko, M.M. and C.P. Reynolds, *Determination of subcutaneous tumor size in athymic (nude) mice.* Cancer Chemother Pharmacol, 1989. **24**(3): p. 148-54.
144. Chen, S., et al., *fastp: an ultra-fast all-in-one FASTQ preprocessor.* Bioinformatics, 2018. **34**(17): p. i884-i890.
145. Patro, R., et al., *Salmon provides fast and bias-aware quantification of transcript expression.* Nat Methods, 2017. **14**(4): p. 417-419.
146. Soneson, C., M.I. Love, and M.D. Robinson, *Differential analyses for RNA-seq: transcript-level estimates improve gene-level inferences.* F1000Res, 2015. **4**: p. 1521.
147. Ritchie, M.E., et al., *limma powers differential expression analyses for RNA-sequencing and microarray studies.* Nucleic Acids Res, 2015. **43**(7): p. e47.
148. Dai, M., et al., *Evolving gene/transcript definitions significantly alter the interpretation of GeneChip data.* Nucleic Acids Res, 2005. **33**(20): p. e175.
149. Butler, A., et al., *Integrating single-cell transcriptomic data across different conditions, technologies, and species.* Nature Biotechnology, 2018. **36**(5): p. 411-420.
150. Becht, E., et al., *Dimensionality reduction for visualizing single-cell data using UMAP.* Nature Biotechnology, 2019. **37**(1): p. 38-44.
151. Smyth, G.K., *limma: Linear Models for Microarray Data*, in *Bioinformatics and Computational Biology Solutions Using R and Bioconductor*, R. Gentleman, et al., Editors. 2005, Springer New York: New York, NY. p. 397-420.

Fig 1

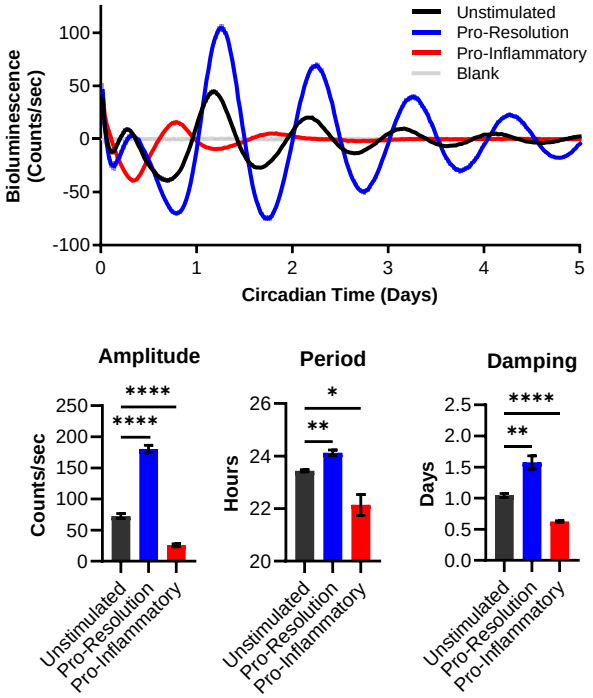
Unstimulated
Pro-Resolution
Pro-Inflammatory
Blank
Bioluminescence (Counts/sec)
100
50
0
-50
-100
0
1
2
3
4
5
Circadian Time (Days)
Amplitude
Counts/sec
250
200
150
100
50
0
****
****
Period
Hours
26
24
22
20
*
**
Damping
Days
2.5
2.0
1.5
1.0
0.5
0.0
****
**
Unstimulated
Pro-Resolution
Pro-Inflammatory

Fig 2

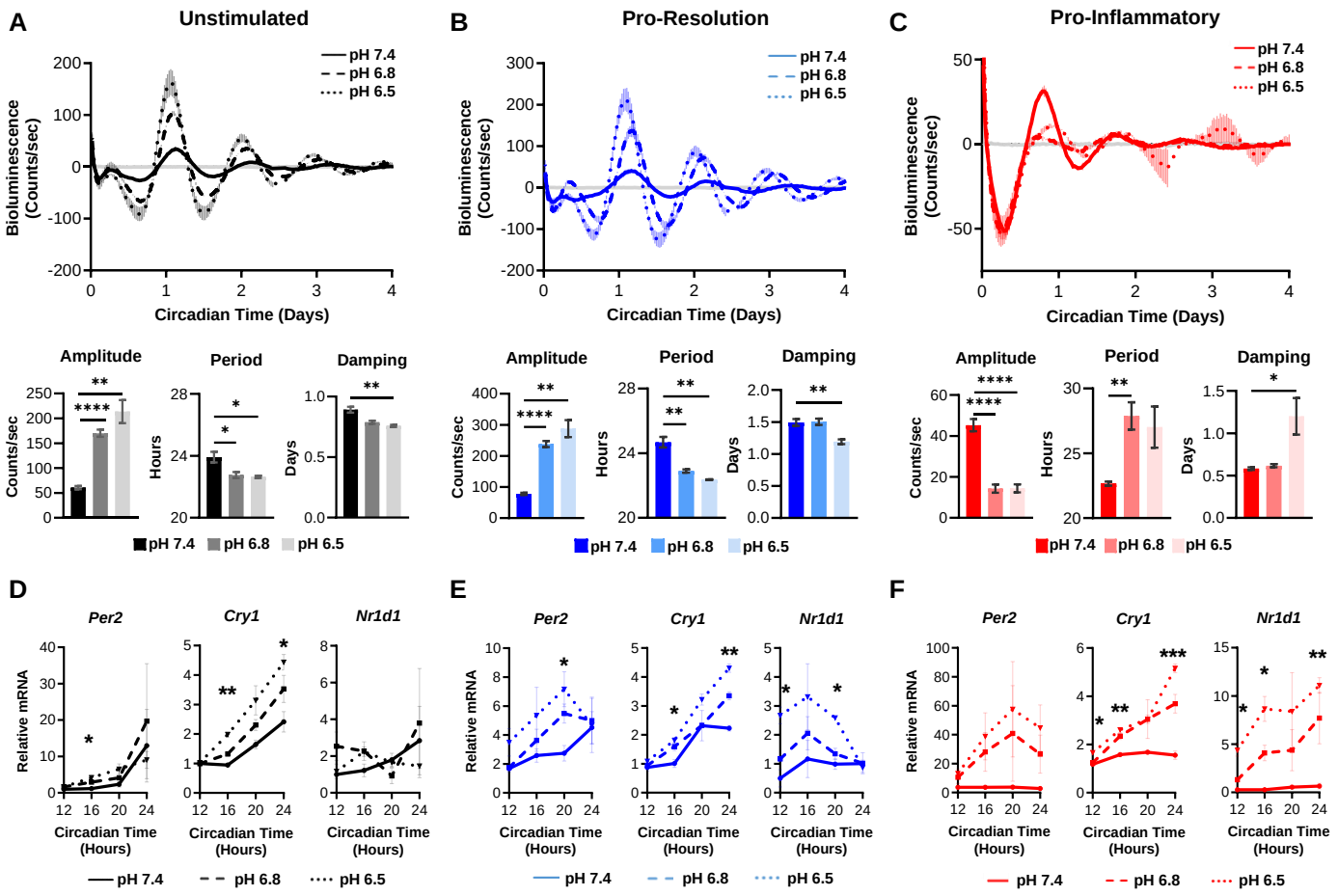
A
Unstimulated
pH 7.4
pH 6.8
pH 6.5
Bioluminescence (Counts/sec)
Circadian Time (Days)
B
Pro-Resolution
C
Pro-Inflammatory
Amplitude
Period
Damping
Counts/sec
Hours
Days
D
E
F
Per2
Cry1
Nr1d1
Relative mRNA
Circadian Time (Hours)

Fig 3

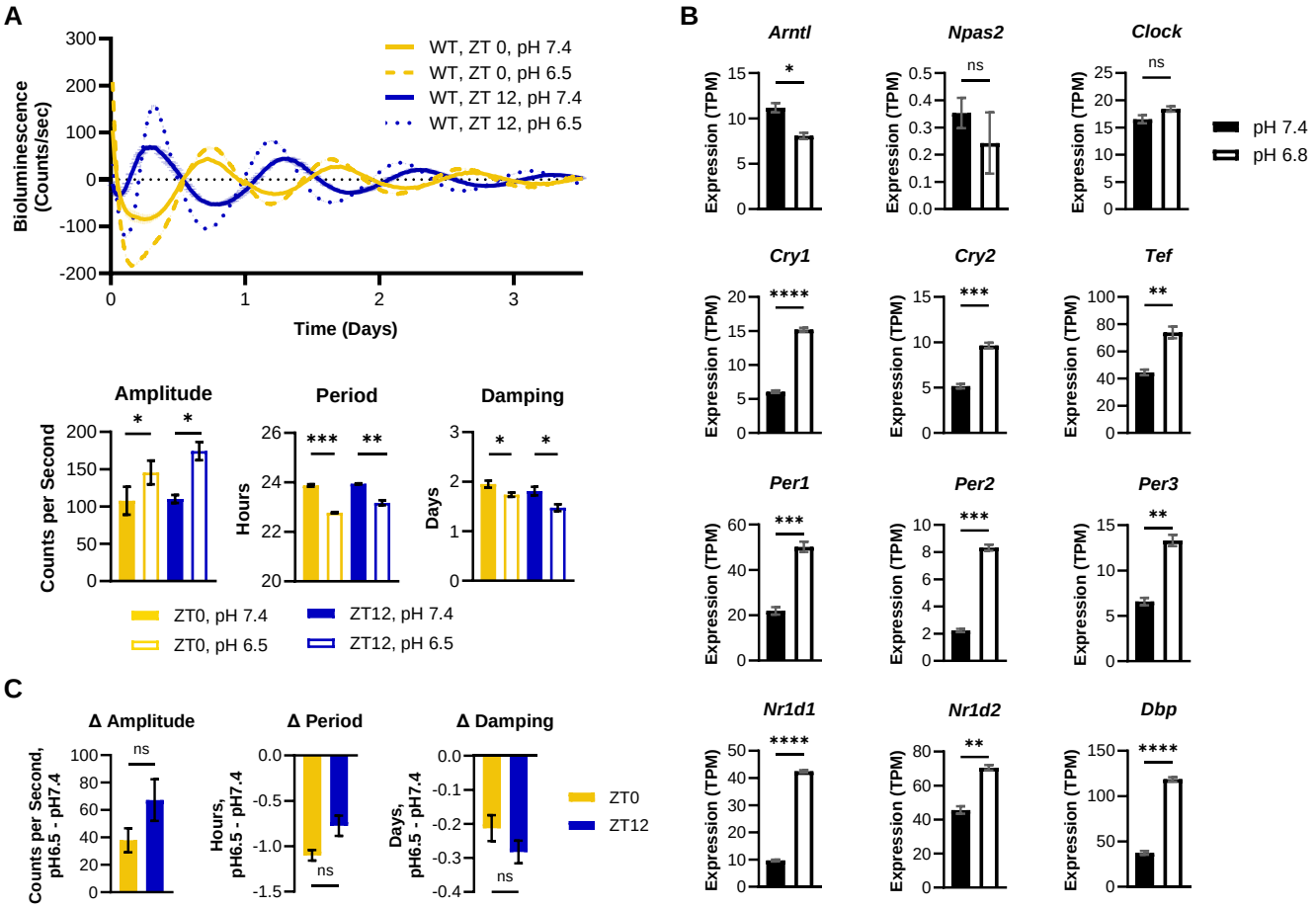
A
Bioluminescence (Counts/sec)
Time (Days)
WT, ZT 0, pH 7.4
WT, ZT 0, pH 6.5
WT, ZT 12, pH 7.4
WT, ZT 12, pH 6.5
Amplitude
Period
Damping
Counts per Second
Hours
Days
ZT0, pH 7.4
ZT0, pH 6.5
ZT12, pH 7.4
ZT12, pH 6.5
B
Arntl
Npas2
Clock
Cry1
Cry2
Tef
Per1
Per2
Per3
Nr1d1
Nr1d2
Dbp
Expression (TPM)
pH 7.4
pH 6.8
C
Δ Amplitude
Δ Period
Δ Damping
Counts per Second, pH6.5 - pH7.4
Hours, pH6.5 - pH7.4
Days, pH6.5 - pH7.4
ZT0
ZT12

Fig 4

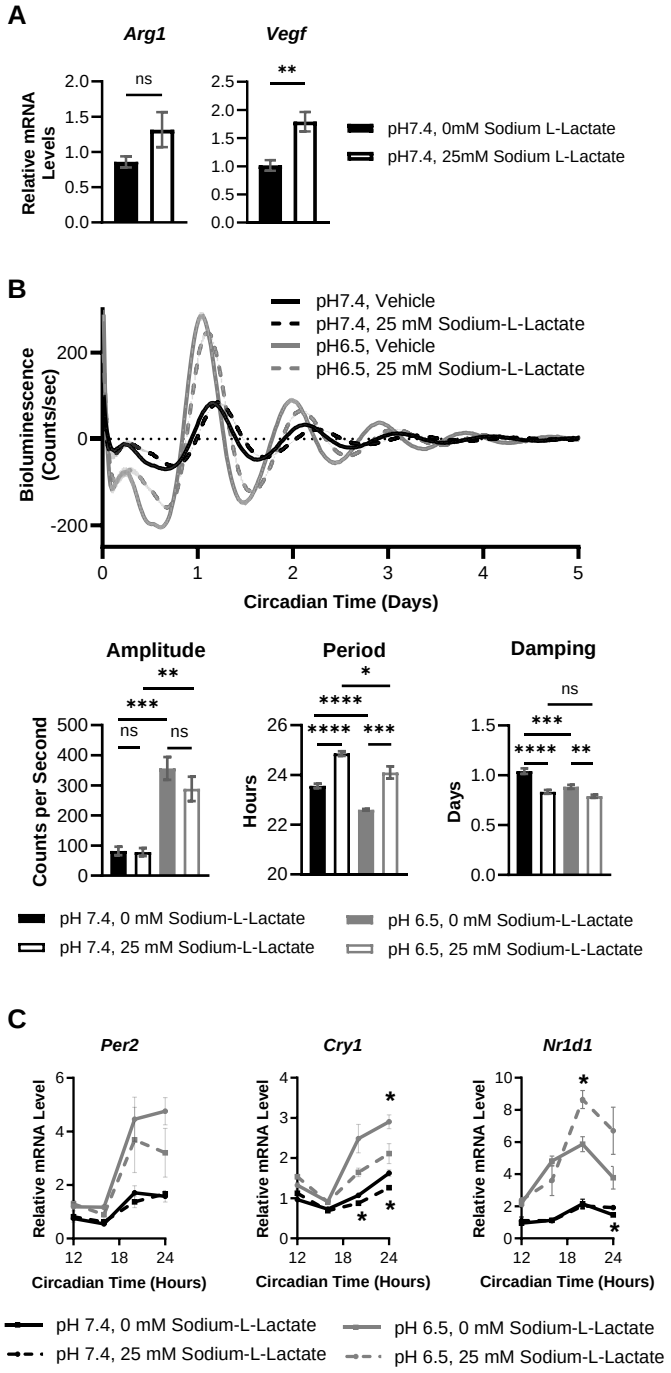
A
Arg1
Vegf
Relative mRNA Levels
ns
**
pH7.4, 0mM Sodium L-Lactate
pH7.4, 25mM Sodium L-Lactate
B
pH7.4, Vehicle
pH7.4, 25 mM Sodium-L-Lactate
pH6.5, Vehicle
pH6.5, 25 mM Sodium-L-Lactate
Bioluminescence (Counts/sec)
Circadian Time (Days)
Amplitude
Period
Damping
Counts per Second
Hours
Days
pH 7.4, 0 mM Sodium-L-Lactate
pH 7.4, 25 mM Sodium-L-Lactate
pH 6.5, 0 mM Sodium-L-Lactate
pH 6.5, 25 mM Sodium-L-Lactate

C
Per2
Cry1
Nr1d1
Relative mRNA Level
Circadian Time (Hours)
pH 7.4, 0 mM Sodium-L-Lactate
pH 7.4, 25 mM Sodium-L-Lactate
pH 6.5, 0 mM Sodium-L-Lactate
pH 6.5, 25 mM Sodium-L-Lactate

Fig 5

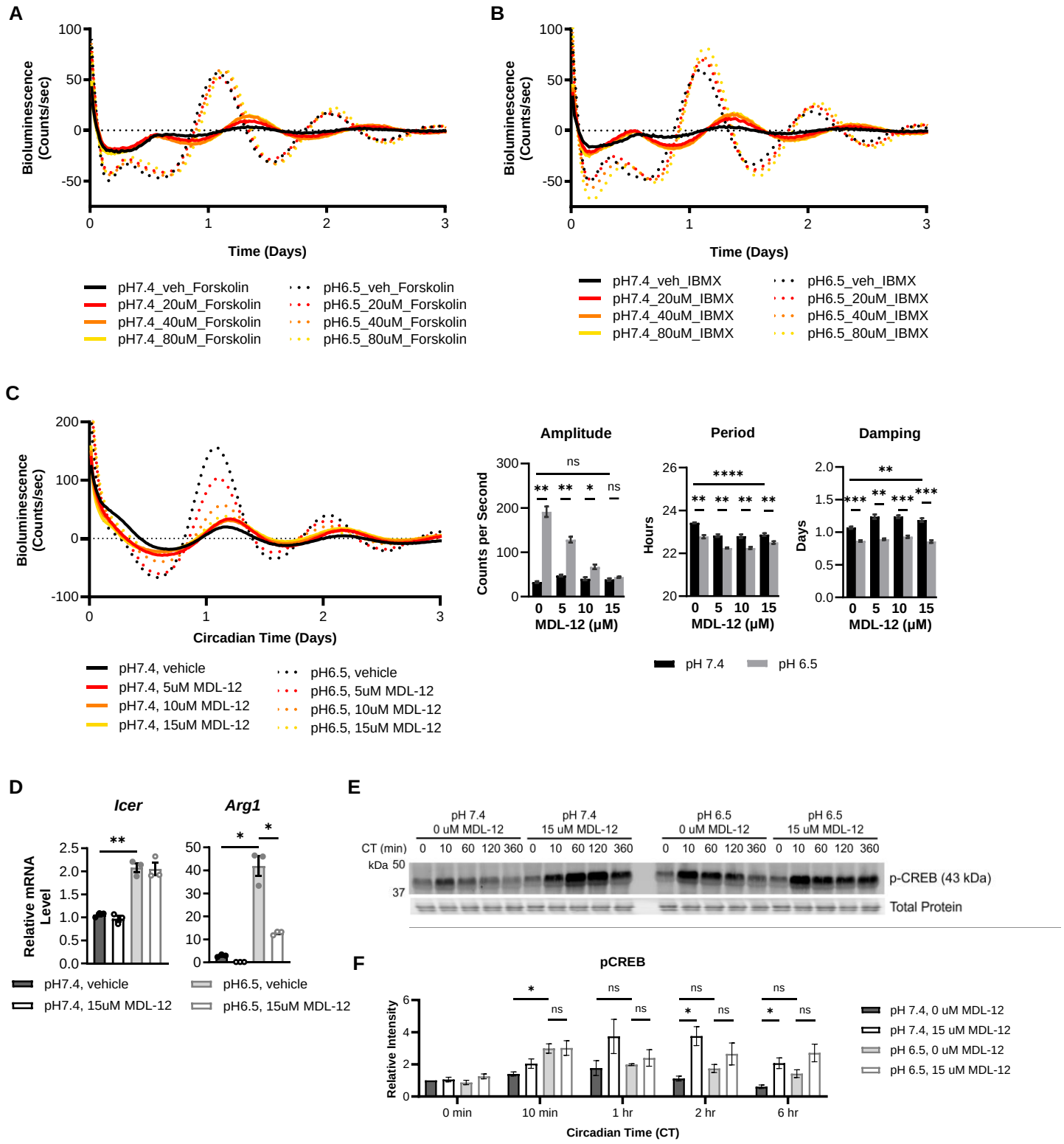
A
Bioluminescence (Counts/sec)
Time (Days)
pH7.4_veh_Forskolin
pH7.4_20uM_Forskolin
pH7.4_40uM_Forskolin
pH7.4_80uM_Forskolin
pH6.5_veh_Forskolin
pH6.5_20uM_Forskolin
pH6.5_40uM_Forskolin
pH6.5_80uM_Forskolin
B
Bioluminescence (Counts/sec)
Time (Days)
pH7.4_veh_IBMX
pH7.4_20uM_IBMX
pH7.4_40uM_IBMX
pH7.4_80uM_IBMX
pH6.5_veh_IBMX
pH6.5_20uM_IBMX
pH6.5_40uM_IBMX
pH6.5_80uM_IBMX
C
Bioluminescence (Counts/sec)
Circadian Time (Days)
pH7.4, vehicle
pH7.4, 5uM MDL-12
pH7.4, 10uM MDL-12
pH7.4, 15uM MDL-12
pH6.5, vehicle
pH6.5, 5uM MDL-12
pH6.5, 10uM MDL-12
pH6.5, 15uM MDL-12
Amplitude
Counts per Second
MDL-12 (μM)
Period
Hours
MDL-12 (μM)
Damping
Days
MDL-12 (μM)
pH 7.4
pH 6.5
D
Icer
Arg1
Relative mRNA Level
pH7.4, vehicle
pH7.4, 15uM MDL-12
pH6.5, vehicle
pH6.5, 15uM MDL-12
E
pH 7.4 0 uM MDL-12
pH 7.4 15 uM MDL-12
pH 6.5 0 uM MDL-12
pH 6.5 15 uM MDL-12
CT (min)
kDa
p-CREB (43 kDa)
Total Protein
F
pCREB
Relative Intensity
0 min
10 min
1 hr
2 hr
6 hr
Circadian Time (CT)
pH 7.4, 0 uM MDL-12
pH 7.4, 15 uM MDL-12
pH 6.5, 0 uM MDL-12
pH 6.5, 15 uM MDL-12

Fig 6

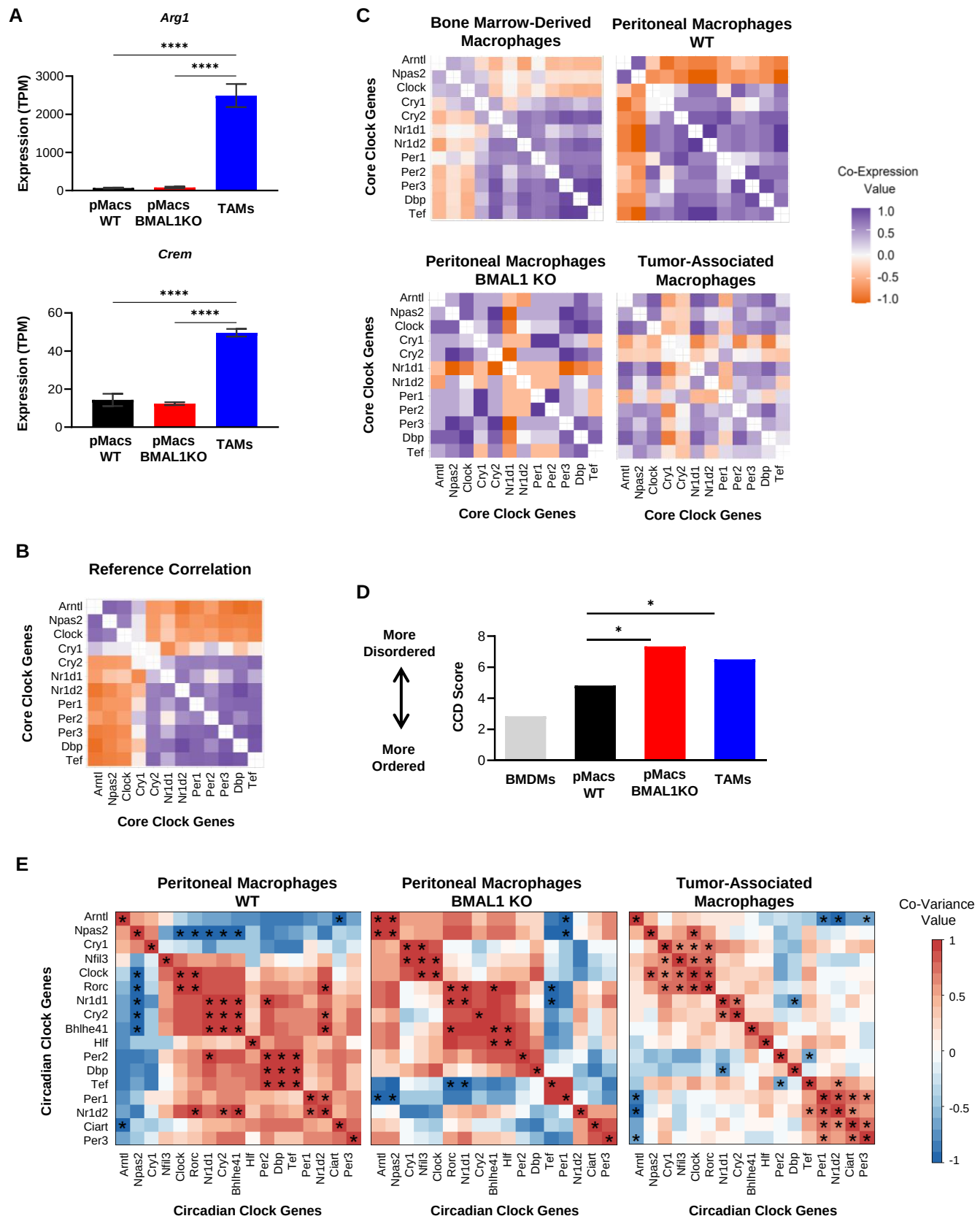
A
Arg1
****
****
Expression (TPM)
3000
2000
1000
0
pMacs WT
pMacs BMAL1KO
TAMs
Crem
****
****
Expression (TPM)
60
40
20
0
pMacs WT
pMacs BMAL1KO
TAMs
C
Bone Marrow-Derived Macrophages
Peritoneal Macrophages WT
Peritoneal Macrophages BMAL1 KO
Tumor-Associated Macrophages
Core Clock Genes
Arntl
Npas2
Clock
Cry1
Cry2
Nr1d1
Nr1d2
Per1
Per2
Per3
Dbp
Tef
Co-Expression Value
1.0
0.5
0.0
-0.5
-1.0
B
Reference Correlation
Core Clock Genes
D
More Disordered
More Ordered
CCD Score
8
6
4
2
0
*
*
BMDMs
pMacs WT
pMacs BMAL1KO
TAMs
E
Peritoneal Macrophages WT
Peritoneal Macrophages BMAL1 KO
Tumor-Associated Macrophages
Circadian Clock Genes
Arntl
Npas2
Cry1
Nfil3
Clock
Rorc
Nr1d1
Cry2
Bhlhe41
Hlf
Per2
Dbp
Tef
Per1
Nr1d2
Ciart
Per3
Co-Variance Value
1
0.5
0
-0.5
-1

Fig 7

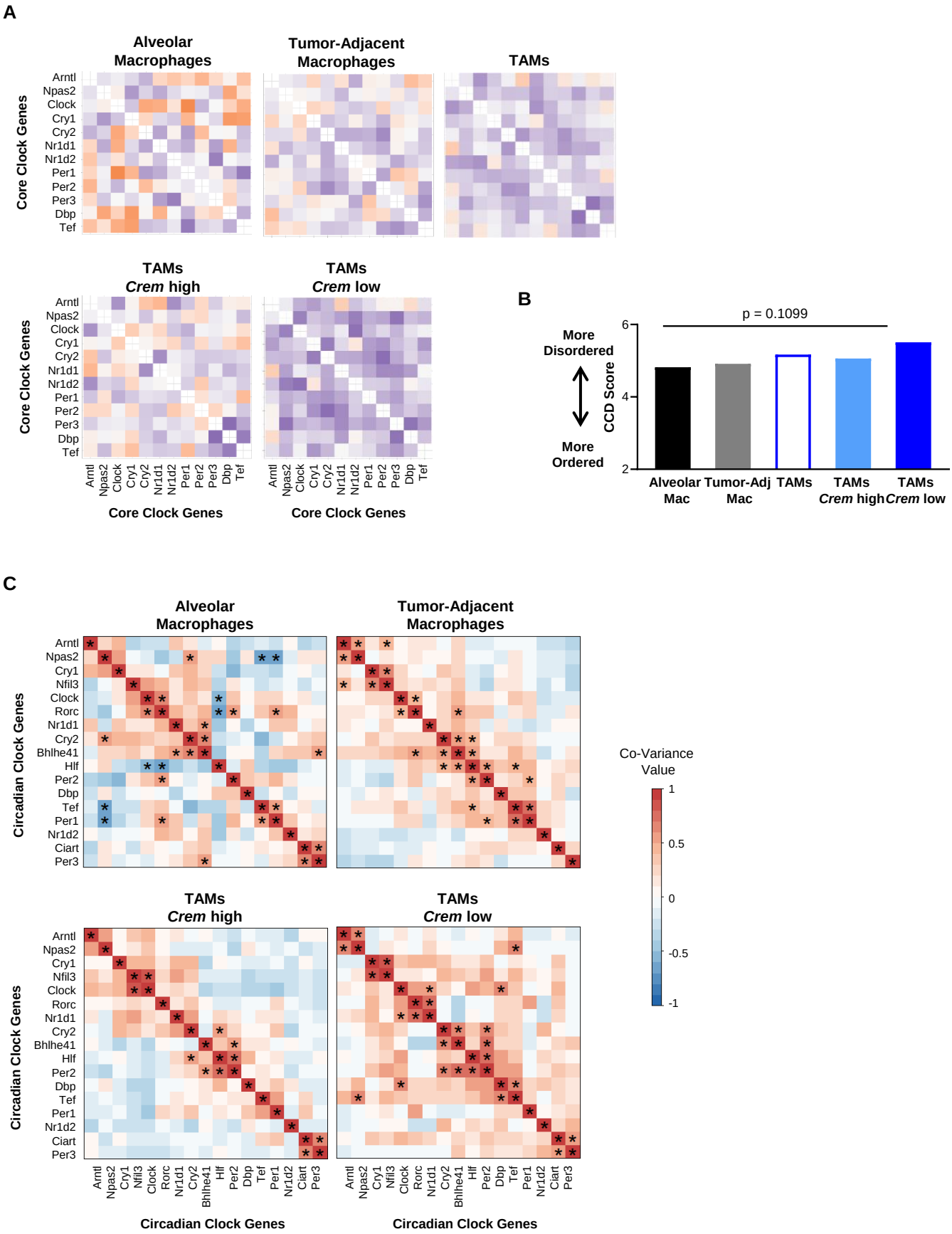
A
Alveolar Macrophages
Tumor-Adjacent Macrophages
TAMs
TAMs *Crem* high
TAMs *Crem* low
Core Clock Genes
Arntl
Npas2
Clock
Cry1
Cry2
Nr1d1
Nr1d2
Per1
Per2
Per3
Dbp
Tef
B
p = 0.1099
More Disordered
More Ordered
CCD Score
6
4
2
Alveolar Mac
Tumor-Adj Mac
TAMs
TAMs *Crem* high
TAMs *Crem* low
C
Circadian Clock Genes
Nfil3
Ciart
Co-Variance Value
1
0.5
0
-0.5
-1

Fig 8

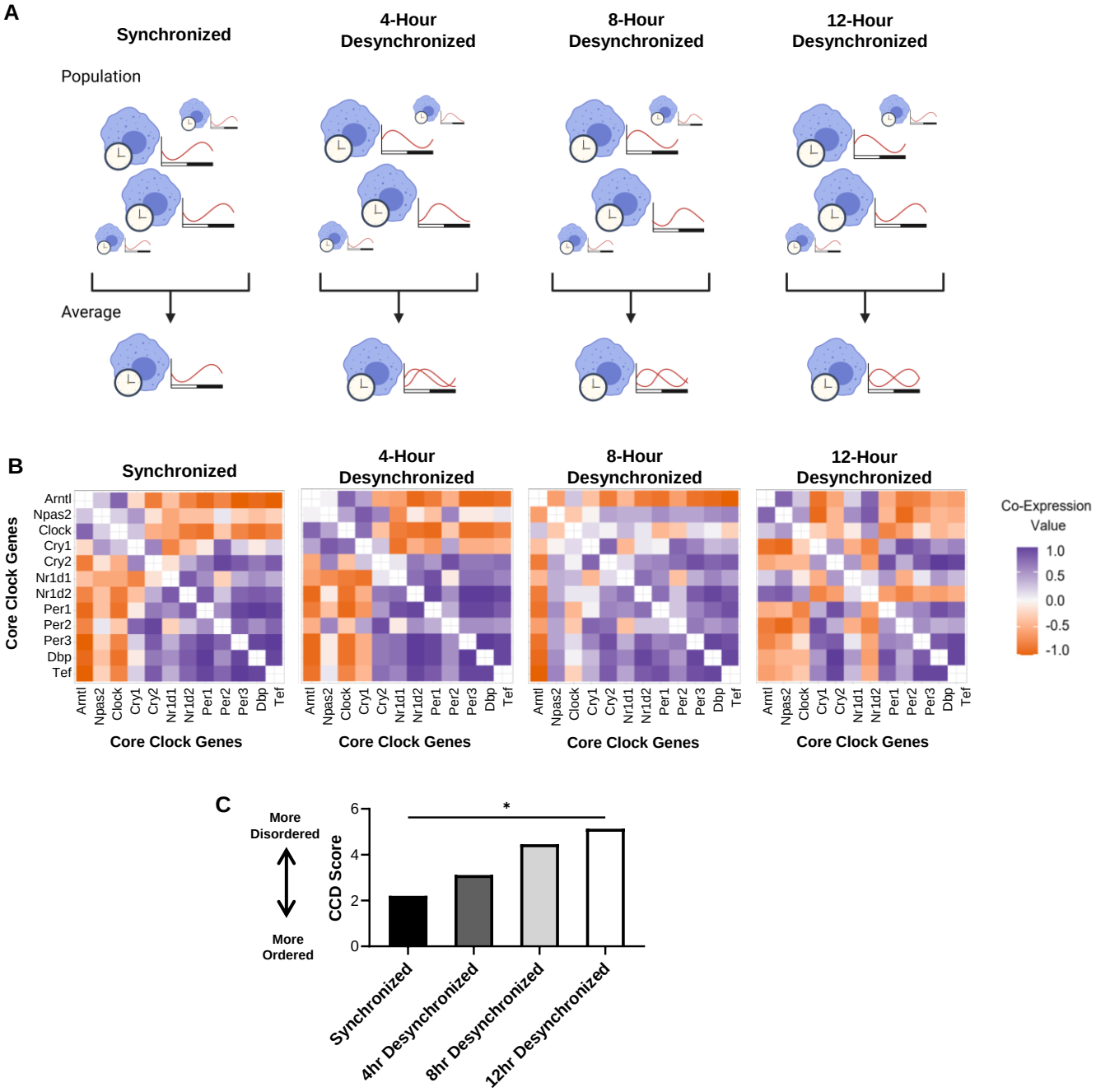
A
Synchronized
4-Hour Desynchronized
8-Hour Desynchronized
12-Hour Desynchronized
Population
Average
B
Synchronized
4-Hour Desynchronized
8-Hour Desynchronized
12-Hour Desynchronized
Core Clock Genes
Arntl
Npas2
Clock
Cry1
Cry2
Nr1d1
Nr1d2
Per1
Per2
Per3
Dbp
Tef
Core Clock Genes
Co-Expression Value
1.0
0.5
0.0
-0.5
-1.0
C
More Disordered
More Ordered
CCD Score
0
2
4
6
*
Synchronized
4hr Desynchronized
8hr Desynchronized
12hr Desynchronized

Fig 9

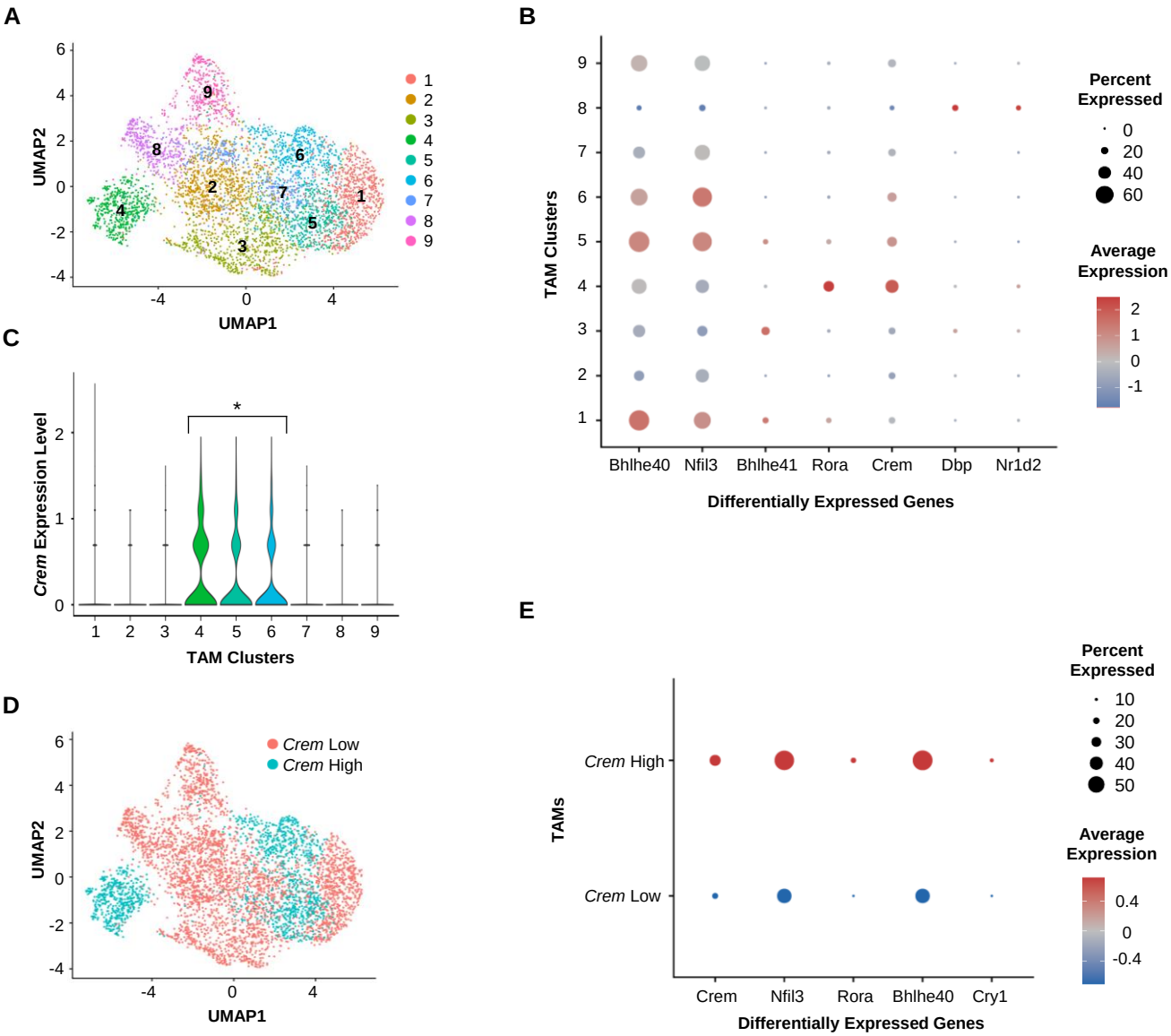
A
UMAP2
UMAP1
1
2
3
4
5
6
7
8
9
B
TAM Clusters
Bhlhe40
Nfil3
Bhlhe41
Rora
Crem
Dbp
Nr1d2
Differentially Expressed Genes
Percent Expressed
0
20
40
60
Average Expression
2
1
0
-1
C
Crem Expression Level
TAM Clusters
*
D
Crem Low
Crem High
UMAP2
UMAP1
E
TAMs
Crem High
Crem Low
Crem
Nfil3
Rora
Bhlhe40
Cry1
Differentially Expressed Genes
Percent Expressed
10
20
30
40
50
Average Expression
0.4
0
-0.4

Fig 10

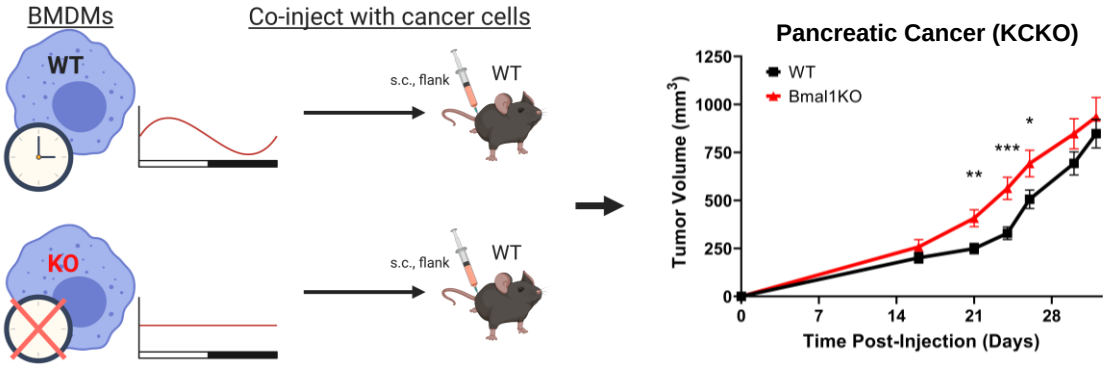
BMDMs
Co-inject with cancer cells
WT
KO
s.c., flank
WT
s.c., flank
WT
Pancreatic Cancer (KCKO)
WT
Bmal1KO
Tumor Volume (mm3)
1250
1000
750
500
250
0
0
7
14
21
28
Time Post-Injection (Days)
**
***
*